Bachelor Thesis

Degree Project in
Earth Science 15 hp

Kinematic analysis of nappe contacts in the Olympos-Ossa and Pelion regions, Greece: Implications for the tectonic evolution of the Cycladic Blueschist Unit

Joshua Gaudy

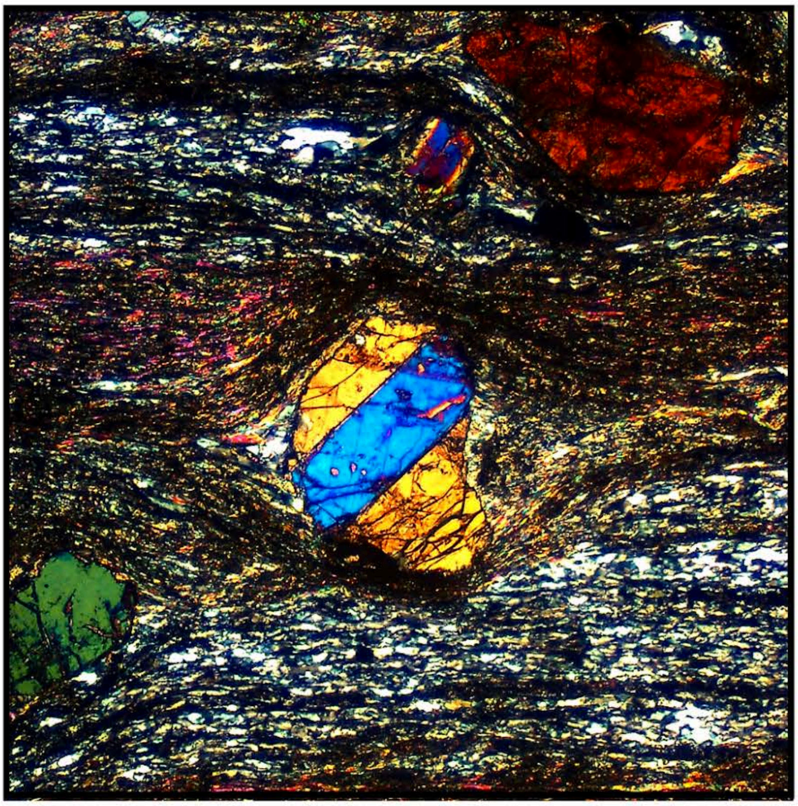

Abstract

Stockholm 2024

Department of Geological Sciences
Stockholm University
SE-106 91 Stockholm

This study conducts a kinematic analysis of the nappe contacts that are found in the Olympos-Ossa, Pelion and Skiathos regions of Greece with a focus on the Cycladic Blueschist Unit (CBU). The analysis focused on microstructures in thin sections to determine the shear sense and its correlation to mineral assemblages and tectonic contacts. Samples from the Olympos Ossa region showed a general top-SW shear sense, corresponding to a blueschist and greenschist-facies metamorphism and the isolation of the Upper-CBU. The Pelion region exhibited, exhibited both top-SW and top-NE shearing, with a possible correlation between the top-SW movement of the Olympos-Ossa region. While the top-NE shearing cut out the overlying Pelagonian units through early Miocene extensional faulting. The Upper Pelagonian Unit and Eohellenic Unit on Skiathos, tectonically stripped from the Pelion region reflect the metamorphic conditions and deformation history before their removal on Pelion

Keywords

Cycladic Blueschist Unit, CBU, Olympos-Ossa, Pelion, Skiathos, kinematic analysis, Nappe, Microstructures, shear sense

Contents

1 Introduction

The investigation of microtectonics is essential for the interpretation of deformational history and tectonic evolution in orogenic belts (Graveleau et al., 2012), where significant deformation and metamorphism are commonly observed due to processes like subduction, continental collision, and extension (Ganne et al., 2006; Jolivet et al., 2003).

An orogenic belt linked to subduction and subsequent large-scale extension is exemplified by the Hellenides in Greece, particularly the Aegean Sea region (Kilias, 2024). The Hellenides, which have been forming since the Jurassic, consist of diverse tectonic units that tectonically young from north to south. Six distinct tectonic units are recognized, each composed of various subunits of nappes (Jolivet and Brun, 2010; Kilias, 2024). The amalgamation of these units took place through subduction-related accretion, advancing intermittently towards the south.

An extensively studied unit is the Cycladic Blueschist Unit (CBU) within the northern Pindos Unit (see further information in the geological setting), renowned as a prime natural research site for investigating well-preserved, subduction-related high-pressure rocks that resurfaced (Lister et al., 1984; Peillod et al., 2021; Ring et al., 2020, 2010). The CBU, extensively examined over recent decades in the Cyclades archipelago (Fig. 1a), experienced significant disruption during the Miocene due to large-scale continental extension following subduction episodes from the Paleocene to the Oligocene (reviews of Jolivet and Brun, 2010; Ring et al., 2010). This disruption led to the formation of the Aegean Sea basin. By contrast, the extensional effects were less pronounced in western mainland Greece, resulting in lesser disturbance relative to high-pressure belts like the CBU. The CBU is also visible in the Olympos-Ossa region and the Pelion Peninsula on the Greek mainland, enabling the study of challenging tectonic contacts with underlying and overlying units, which is not easily achievable in the Cyclades archipelago. While the tectonic evolution in the Cyclades is well-documented, the Olympos-Ossa and Pelion regions provide fresh new perspectives on CBU research (Fig. 2-3).

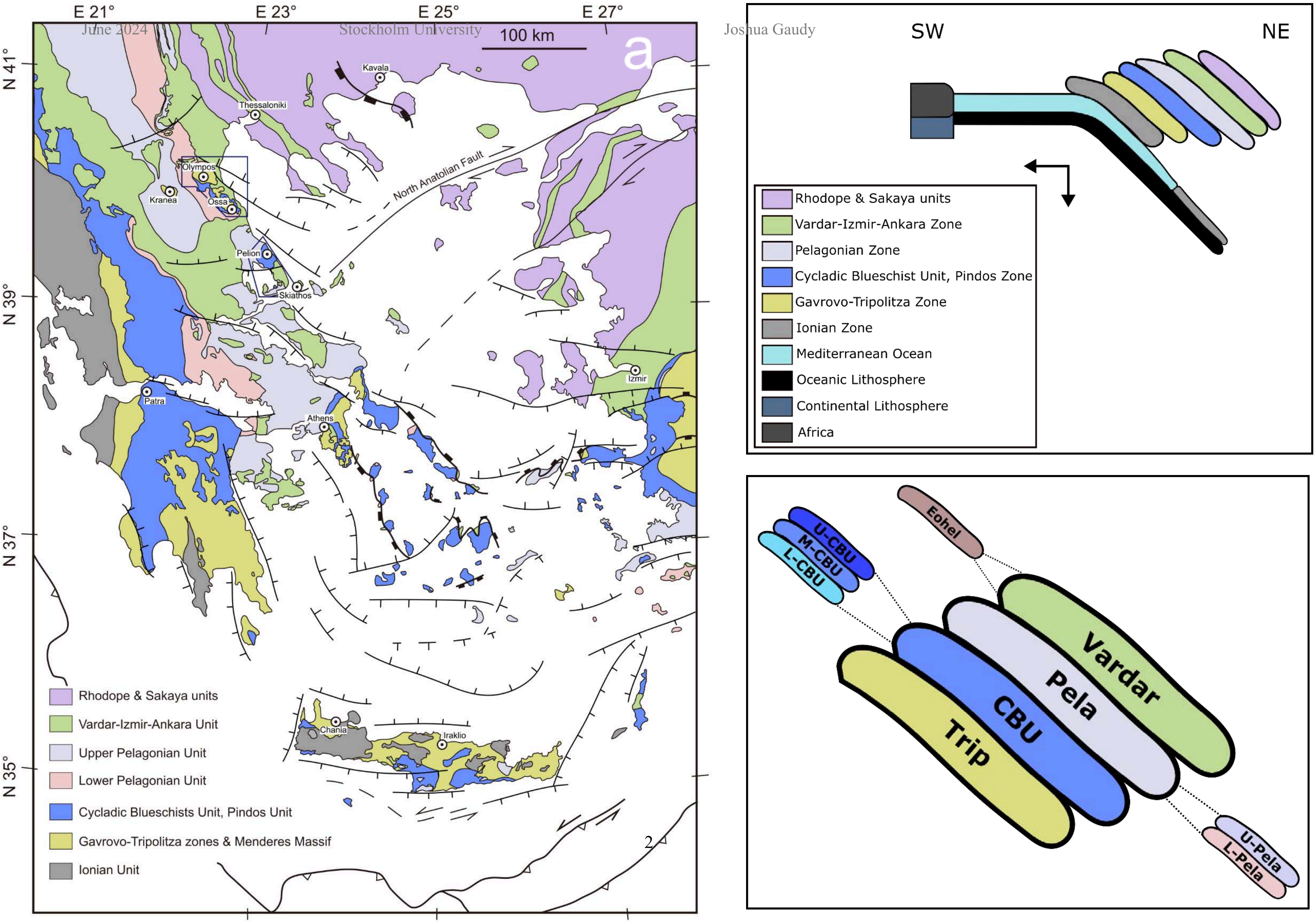
E 21°
E 23°
E 25°
E 27°
N 41°
N 39°
N 37°
N 35°
100 km
a
Kavala
Thessaloniki
North Anatolian Fault
Olympos
Kranea
Ossa
Pelion
Skiathos
Izmir
Patra
Athens
Chania
Iraklio
Rhodope & Sakaya units
Vardar-Izmir-Ankara Unit
Upper Pelagonian Unit
Lower Pelagonian Unit
Cycladic Blueschists Unit, Pindos Unit
Gavrovo-Tripolitza zones & Menderes Massif
Ionian Unit
SW
NE
Rhodope & Sakaya units
Vardar-Izmir-Ankara Zone
Pelagonian Zone
Cycladic Blueschist Unit, Pindos Zone
Gavrovo-Tripolitza Zone
Ionian Zone
Mediterranean Ocean
Oceanic Lithosphere
Continental Lithosphere
Africa
U-CBU
M-CBU
L-CBU
Eohel
Vardar
Pela
CBU
Trip
U-Pela
L-Pela

Figure. 1: (a) A Geological map over the Hellenides showing the different units and nappes. (b) A very simplified SW-NE cross-section illustrating the nappe stacks and the current retreating subduction zone. (c) A simplified illustration of the nappe stacks relevant to this study. These include from top to bottom: the Vardar-Izmir-Ankara Unit with the Eohellenic sub-nappe, the Pelagonian Unit with its upper and lower sub nappes, the Cycladic Blueschist Unit with its upper, middle, lower sub nappes, and the Tripolitza Unit.

2 Geological setting

2.1 Aegean Sea Region

The Aegean Sea region is known for its retreating subduction zone (Ring and Layer, 2003). Unlike advancing subduction zones, retreating subduction zones involve the subducting plate moving away from the overriding plate, causing the subduction zone to migrate oceanward. This often causes large-scale extension of the upper plate behind the subduction zone. Studying its tectonic evolution is challenging as many regions of large-scale extension are under water. During subduction the nappes that make up the Hellenides were stacked (Fig. 1b)(van Hinsbergen et al., 2005). The nappes in the Aegean region form several tectonic zones, which are from the northeast (top) to the southwest (bottom): the Rhodope Unit, the Vardar-Izmir-Ankara Unit (with the Eohellenic Nappe at its top), the Pelagonian Unit, the Pindos Unit with the CBU, the Tripolitza Unit and the Ionian Unit (Fig. 1a-b). Based on structural position, the Pelagonian Unit is subdivided into the Upper and a Lower Pelagonian Unit (Fig. 1c)(Schmid et al., 2020).

2.2 Cycladic Blueschist Unit

Despite being mostly submerged, the CBU is a well-preserved high-pressure rock unit with three distinct nappes, the lower-, middle- and upper-CBU, which are located in the northernmost part of the Pindos Unit (Glodny and Ring, 2022). Geochronological studies concluded that the ages of the nappes span from 53-47 Ma in the Upper-CBU Nappe, 44-38 Ma in the Middle-CBU Nappe to 33-28 in the Lower-CBU Nappe, which show an age from the structural top to the bottom (Glodny and Ring, 2022). Underthrusting and accretion in the Hellenic subduction zone are thought to be the cause of the CBU nappe stacking. There are two units situated on mainland Greece which are equivalent to the CBU, the Ampelakia Unit (sometimes referred to as Ambelakia Unit) in the Olympos-Ossa region and the Pelion Blueschist Unit (PBU) in the Pelion region. Preliminary Rb-Sr age dating by Hong et al. (IGV PhD student) showed that the Ampelakia Unit and the PBU correspond to the upper-CBU nappe.

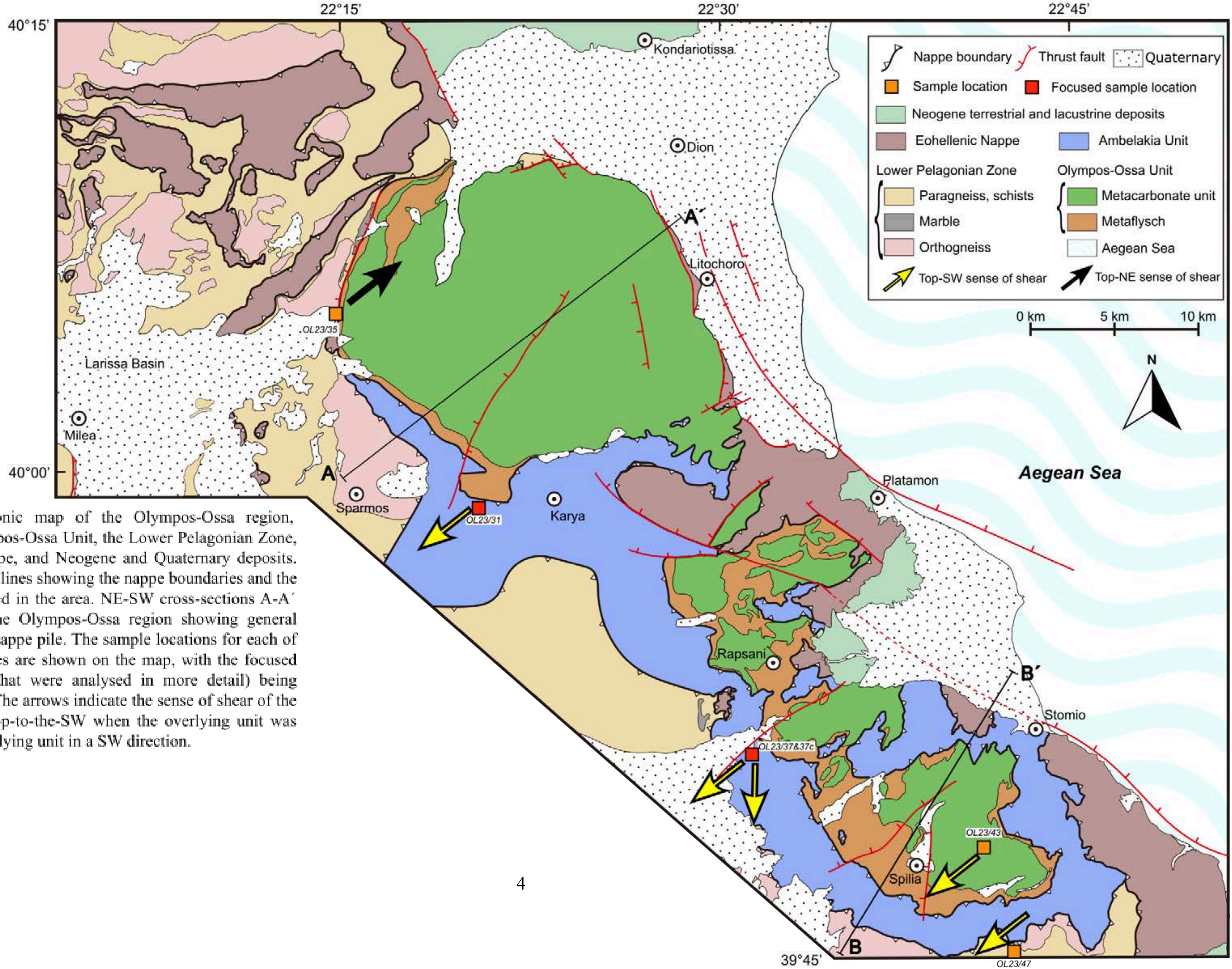

Figure 2: A Tectonic map of the Olympos-Ossa region, including the Olympos-Ossa Unit, the Lower Pelagonian Zone, the Eohellenic Nappe, and Neogene and Quaternary deposits. Alongside these are lines showing the nappe boundaries and the thrust faults recorded in the area. NE-SW cross-sections A-A´ and B-B´ across the Olympos-Ossa region showing general architecture of the nappe pile. The sample locations for each of the analysed samples are shown on the map, with the focused samples (samples that were analysed in more detail) being highlighted in red. The arrows indicate the sense of shear of the tectonic top, i.e., top-to-the-SW when the overlying unit was thrust over its underlying unit in a SW direction.

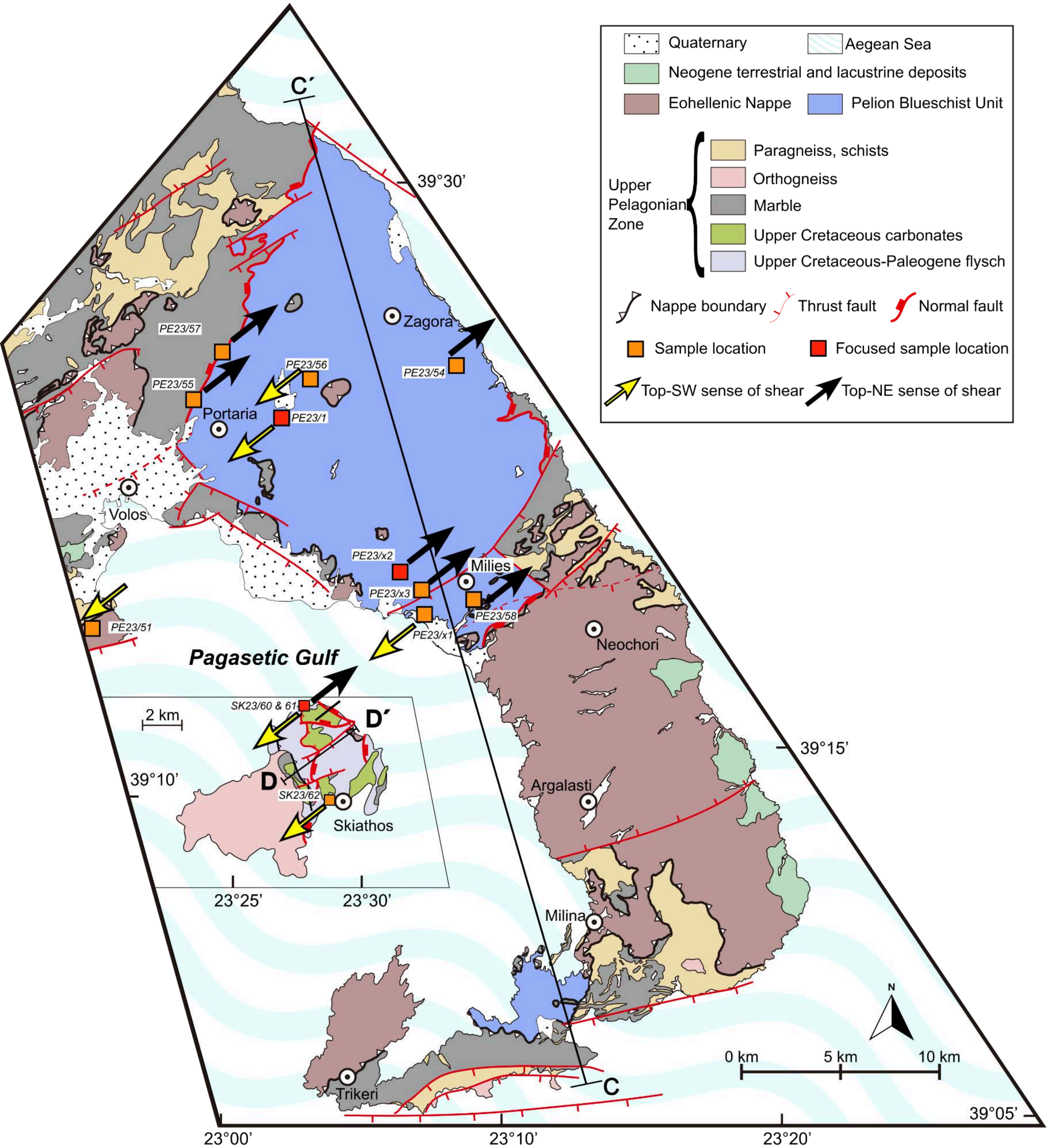

Figure 3: A tectonic map of the Pelion region and Skiathos Island. The present units in this map are the Upper Pelagonian Zone, the Pelion Blueschist Unit (PBU), the Eohellenic Nappe, as well as the Neogene and Quaternary deposits. Note that the Lower Pelagonian Unit is completely missing in the Pelion region. Nappe boundaries, thrust- and normal faults are highlighted. NNW-SSE cross-section C-C′ for the Pelion region and a SW-NE cross section D-D' for Skiathos Island shown. The sample locations for each of the analysed samples are showcased on the map, with the focused samples (samples that were analysed in more detail) being highlighted in red. Alongside these are the directional shear sense arrows either pointing NE-SW.

2.3 Olympos-Ossa Region

In the Olympos-Ossa region, the structural sequence includes (from top to bottom): the Eohellenic Nappe (part of Vardar- Izmir-Ankara Unit), the Pelagonian, the Ampelakia, and the Olympos-Ossa (Tripolitza Unit) units (Fig. 2) (Schermer et al., 1990). The Eohellenic Nappe is characterised by greenschist and amphibolite-facies rocks (Jacobshagen, 1986; Schermer et al., 1990). The Pelagonian Unit in the Olympos-Ossa region encompasses only the Lower Pelagonian Unit overlaying the Ampelakia Unit. The Lower Pelagonian Unit is comprised of pre-Alpine greenschist and sub-blueschist-facies rocks (Schermer, 1993). It in part experienced blueschist and greenschist-facies metamorphism with P/T conditions ranging between 4 to 6 kbar and 350 to 500 °C (Schermer et al., 1990). The dating of this metamorphic overprint is problematic. $^{40}Ar/^{39}Ar$ white mica (Wm) dating provided ages of 61-53 Ma, whereas Rb-Sr Wm ages are 47 to 39 Ma (Schermer et al., 1990). The Ampelakia Unit (CBU) consists of blueschist-facies rocks (Jacobshagen, 1986). The Ampelakia Unit correlates with the upper-CBU nappe (Hong et al., unpublished data). Its blueschist-facies overprint occurred at P-T conditions of 6 to 8 kbar and 200 to 350 °C and is interpreted to be 64-36 Ma (Schermer et al., 1990; Walcott, 1998). The underlying Olympos-Ossa Unit is a Triassic to Eocene carbonate platform with overlying flysch sediments (Godfriaux, 1968; Kilias, 2024). The flysch is mildly high-pressure blueschist-facies metamorphosed with P/T conditions ranging from 5 to 8 kbar and 250 to 350 °C (Schermer et al., 1990). The age of the blueschist-facies overprint is poorly constrained but thought to have ended by 25 Ma. A total of 6 samples were gathered from various units from this region (Table 1).

The structural sequence and the relationships between these units can be seen in the SW-NE cross-sections below (Fig. 4). Cross-section A-A´ traverses over the Olympos region and shows a SW-dipping nappe pile. The Ampelakia Unit as part of the upper-CBU nappe sits directly on flysch of the Tripolitza Unit indicating the middle- and lower-CBU nappes have been tectonically cut out along the contact. (Jacobshagen and Wallbrecher, 1984; Lips et al., 1998). The high-angle normal fault at the NE controlled the exhumation of the Tripolitza Unit and the high-altitude are of Mt Olympos. In the hanging wall of this normal fault, the Eohellenic nappe is preserved Cross-section B-B´ crosses over the Ossa region and has a similar structure to A-A´ apart from only having low angle faults across the entire section and the Eohellenic nappe overlying the Ampelakia unit on the NE side. Furthermore, the flysch that is visible on the SW side is not exposed in the NE.

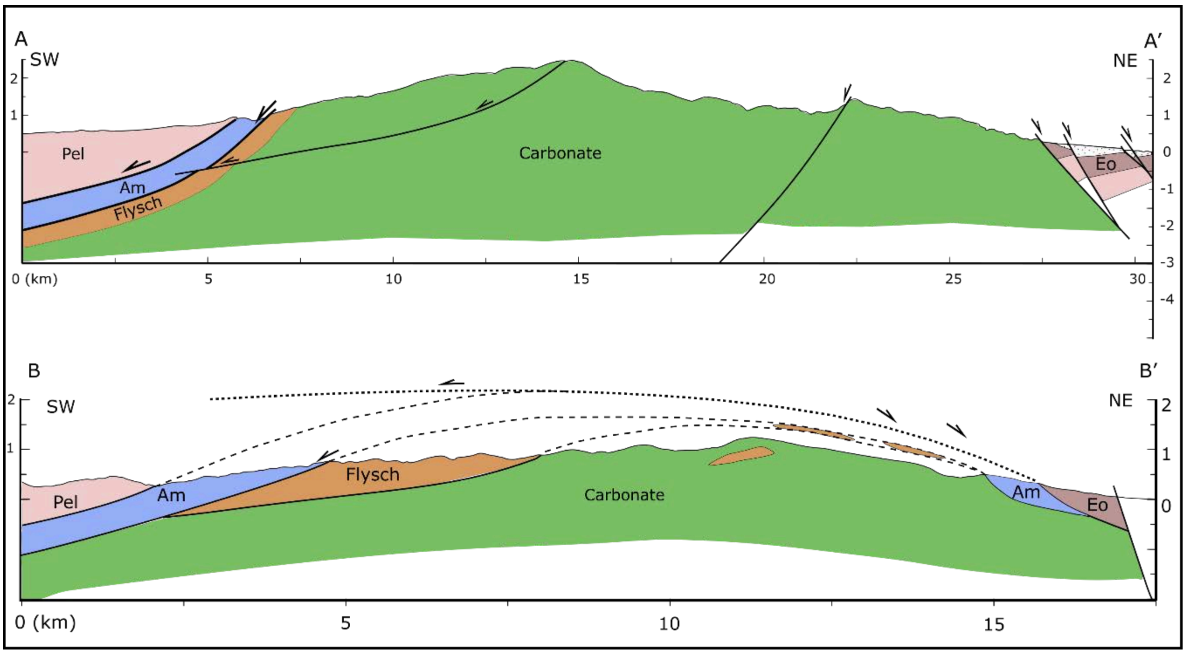

Figure 4: Two cross-sections SW-NE in the Olympos-Ossa region, which contains the units from top to bottom Eohellenic nappe = Eo, Lower Pelagonian = Pel, Ampelakia = Am, Flysch, and Carbonate as seen on Fig. 2. See text for more explanation.

2.4 Pelion Region

The Pelion region has, again from top to bottom, three distinct tectonics units: the Eohellenic Nappe, the Pelagonian Unit and the Pelion Blueschist Unit (PBU) (Fig. 3). The Eohellenic Nappe Unit consists greenschist and amphibolite-facies rocks (Jacobshagen and Wallbrecher, 1984), with P-T conditions of 6 kbar and 200 to 400 °C (Jacobshagen and Wallbrecher, 1984). The Pelagonian Unit in the Pelion region only comprises the Upper Pelagonian Unit, i.e., the entire Lower Pelagonian Unit is missing. The Upper Pelagonian Unit comprises of a pre-Alpine basement overlain by greenschist and sub-greenschist-facies rocks. The PBU is made up by blueschist facies rocks. P-T conditions are estimated at 8 kbar and 350 to 400 °C (Kilias et al., 1995; Lips et al., 1999; Walcott, 1998). The blueschist-facies overprint of the PBU is not well dated. (Hinshaw et al., 2024) reported U-Pb ages of zircon rims of 57 and 53 Ma. Preliminary Rb-Sr dating by Hong et al. corroborates age of 45-53 Ma for the blueschist-facies metamorphism of the PBU. A greenschist-overprint related to an early Miocene extension between 22 and 15 Ma (Hong et al., unpublished data). A total of 10 samples were taken from the Pelion region mostly from the PBU (Table 1).

The cross-section is drawn from the SSE to the NNW to include all units on the peninsula (Fig. 5). i.e., the PBU, Eohellenic nappe and the Upper Pelagonian Unit. A sample from the Eohellenic will not features in the C-C′ cross-section as the sample location is too far away from the cross section (Fig. 3). The PBU is mostly exposed on the NNW side of the cross section covered by small patches of the Eohellenic nappe as well as the Upper Pelagonian Unit. These units have a low-angle tectonic contact above the PBU. Because the Lower Pelagonian Unit, and sometimes the entire Pelagonian Unit is missing along this low angle contact, significant thinning characterizes this contact. As for the SSE side of the cross-section the low angle normal faults separate the PBU from the Upper Pelagonian Unit and the Eohellenic Nappe (Preliminary work Hong).

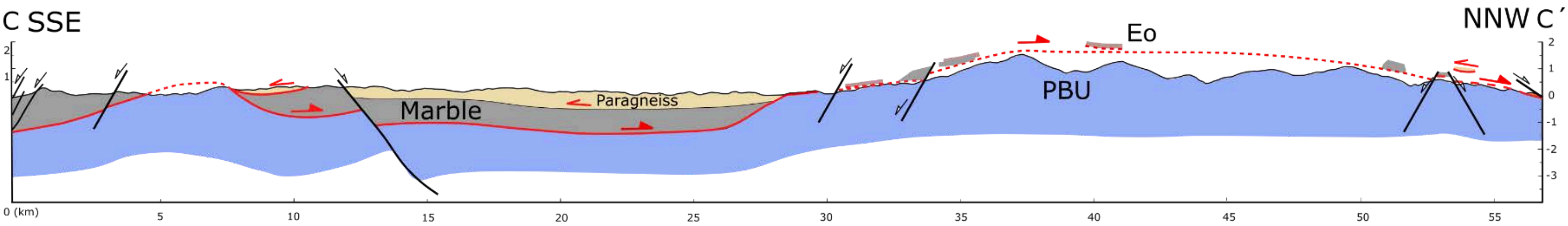

Figure 5: NNE-SSW cross-section C-C′ of the Pelion Region including the PBU, Eohellenic Nappe = Eo and the Lower Pelagonian Unit (Marble and Paragneiss) whereas the Upper Pelagonian Unit is completely missing. The red arrows and lines indicate a low angle fault, while the black arrows and lines show high angle normal faults.

2.5 Skiathos Island

Skiathos Island on the south-eastern side of the Pelion region is dominated by the Upper Pelagonian Unit. A small patch of Eohellenic Unit outcrop on the north-eastern part of the Island (Fig. 3,6)(Porkoláb et al., 2019) and consists of greenschist-facies rocks(Ferentinos, 1973). Both units only show multiple lower greenschist-facies metamorphism events (Ferentinos, 1973; Porkoláb et al., 2020). These metamorphic events are differentiated by their top-Ne or top-SW shearing. The sequence on Skiathos, exposes the Upper Pelagonian Unit and the Eohellenic unit that have been stripped of from the Pelion region. This can provide insights into how the units were deformed on Pelion before they were removed. Three samples were taken in this region, two were gathered from the same location by a carbonates and flysch boundary, while the other was sampled from the flysch close to Skiathos Town (Table 1, Fig. 3).

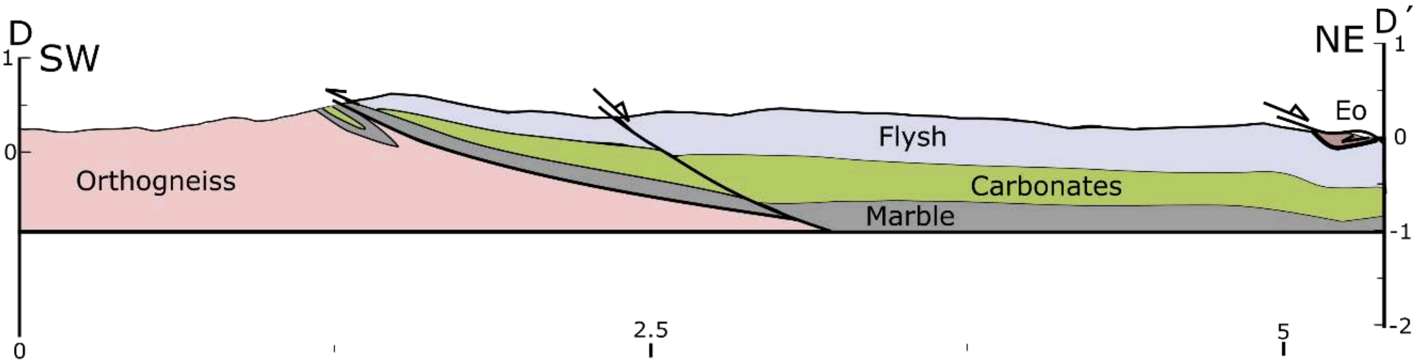

Figure 6: Cross-section D-D´ crossing Skiathos from the SW-NE including the dominant Upper Pelagonian Unit (Carbonates, Flysch, Orthogneiss), Triassic-Jurassic marble and the Eohellenic Nappe. The black arrows indicate thrusts or normal faults.

3 Project Aims

This study aims to systematically analyse 19 thin sections from the Olympos-Ossa, Pelion and Skiathos regions to constrain the shears sense and its relation to the mineral assemblage and the tectonic contacts. Microstructures are the focus of this study. Specifically, shear sense and the relation of the shear zone relative to a geographic reference frame are analysed. Correlation of the shear sense, coordinates, and geographical orientation of each individual sample along with a geological map will allow for better understanding of the structural evolution of the Olympos-Ossa, Pelion and Skiathos regions.

Furthermore, microstructures and mineral assemblages of the individual sample will be compared with the other samples, minerals identified in foliations, and shearing structures are analysed. Through these observations, approximations of metamorphic conditions and deformational history will be concluded, offering deeper insights into the metamorphic evolution of the different regions. The CBU will be the focus of this study.

4 Method

20 thin sections were provided by my supervisor, 19 of which were analysed. The rock samples were collected in 2023 from Greece and made into thin section in the thin section lab 15 Rue Bicquilley, 54200 Toul, France. The sample preparation techniques followed the procedures outlined by the lab.

A Leica DMLSP microscope was used to study the samples. This microscope is outfitted with both plane-polarized light (PPL) and crossed-polarized light (XPL) filter, as well as 2.5x, 10x, 20x and 40x magnification. A micro-diascope for thin sections (MINOX PetroScope) with PPL and XPL filters was used for observing macro scale structures present in the thin sections.

The identified microstructures are described in detail below and descriptions of microstructures present in the samples are provided in the *Results*. A general sample overview containing sample information, rock type, metamorphic grade, mineral assemblage, shear sense indicators, and metamorphic structures were recorded (Table 1). The shear sense was also recorded and later compared to the supervisors' observations to ensure accuracy. Shear sense data (dextral/sinistral) and geographic orientations (NE-SW) which are indicated on each thin section were compared to understand the directional shear sense. The resulting data was then utilized to add directional markers adjacent to appropriate sample coordinates in a map of the relevant areas and cross-sections provided by Hong (unpublished data)., which were adjusted and refined in Inkscape 1.3.2.

The minerals with higher metamorphic grade in each region are being analysed in more detail and are referred to as “focused” samples in figures and text.

Images of noteworthy microstructures and minerals were captures using a Leica MC170 HD camera and recorded with Las Ez. Full-scan images of each thin section were captured using a Nikon Super Coolscan 9000 ED scanner.

4.1 Minerology and Petrology

The analysed samples record blueschist-facies metamorphism that was overprinted by greenschist-facies metamorphism. Based on their mineral assemblage, 14 samples would classify as greenschist-facies rocks and five samples as blueschist-facies rocks. They are described in detail below.

4.1.1 Greenschist

Greenschist-facies rocks are a very common occurrence through the regions and either metabasites or metapelites (Fig. 7)(Glodny and Ring, 2022; Hinshaw et al., 2023; Porkoláb et al., 2019). The mineral composition of metabasic greenschists are different that of metapelitic greenschists. While minerals such as quartz, white mica (Wm), chlorite, and feldspar are found in both protoliths, minerals such as epidote or actinolite are more commonly found in mafic protolith.

4.1.2 Blueschist

Blueschist-facies rocks are higher metamorphic facies than greenschists (Fig. 7) and are less common in the studied area compared to greenschist-facies rocks. Most blueschists are, by contrast, found in the CBU (Laurent et al., 2018; Peillod et al., 2021). Common minerals found in both mafic and pelitic protoliths include blue amphiboles, epidote and quartz. Metabasic blueschist contain mafic minerals such as feldspars and epidote, which are likely not present in metapelitic blueschists (Guiraud et al., 1990)

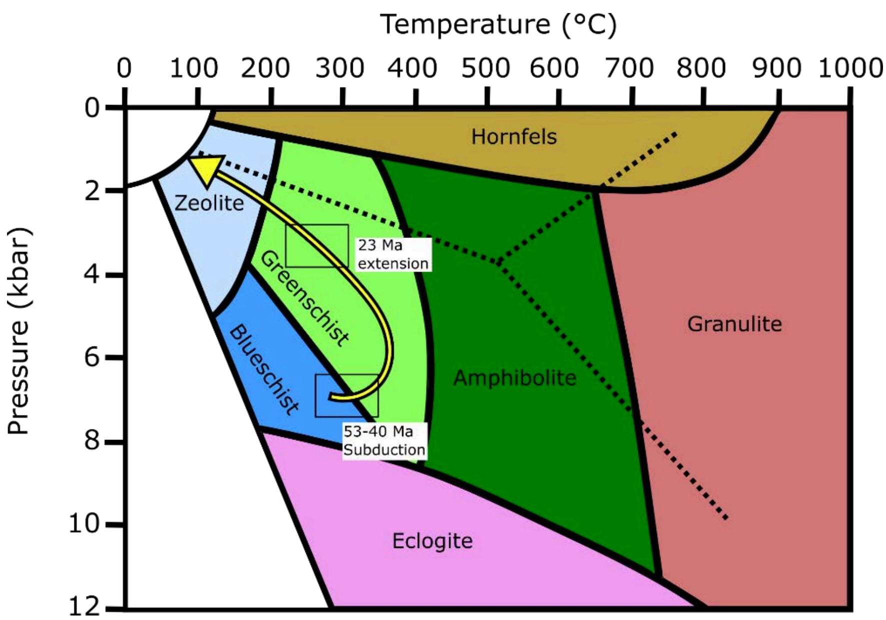

Figure 7: Metamorphic P/T facies diagram to showcase the P/T properties of Greenschists and Blueschists. The schematic P/T path reflects the general metamorphic evolution of the studied rocks. (Winkler, 1976).

4.2 Microstructures and Shear Sense Indicators

The following background on microstructures and shear sense indicators have been adapted from the Microtectonics textbook (Passchier and Trouw, 2005) and Introduction to Metamorphic Textures and

Microstructures (Barker, 1998) to only include structures observed in the studied samples. An illustration of every microstructure that are featured in this study is available in Figure 8.

4.2.1 Foliations

The foliation in the studied samples is secondary tectonometamorphic foliations, which do not preserve sedimentary relics, but do preserve mafic minerals. Mylonitic foliation is defined as strongly recrystallized matrix-minerals with small grain size.

4.2.2 Porphyroclasts

Porphyroclasts are pre-existing, large, single crystals or rounded polycrystalline fragments in a mylonitic matrix. Common minerals that form porphyroclasts are felspar, pyroxene, garnet, Wm, and hornblende. Porphyroclasts in the samples are usually deformed as mantled porphyroclasts or porphyroclasts with strain shadows. In mantled porphyroclasts, the centre crystal has a fine-grained rim of the same composition. Strain shadows around porphyroclasts are composed of a different material than the porphyroclast in the centre. Porphyroclasts often form asymmetric wings that are reliable shear sense indicators. As mantled porphyroclasts distort, the wings distort as well and are distinguished into ϕ-type, σ-type, and δ-type. σ-type and δ-type have an asymmetrical symmetry and can be used as a shear sense indicator. By contrast ϕ-type, which is symmetrical and can, therefore, not be used as an indicator. In the case of porphyroclasts with strain shadows the sense of shear is harder to determine due to the deformation of the strain shadows not being as pronounced as the mantled porphyroclasts. Otherwise, the determination of shear sense for strain shadows are akin to the deformation of σ-type mantled porphyroclasts. Due to their similarities these two variants are often hard to distinguish.

4.2.3 Porphyroblasts

Not to be confused with porphyroclasts, porphyroblasts are large, single crystals formed by metamorphic growth, with inclusions of other minerals. The most common porphyroblasts are alumino-silicates found in metapelites. In this study, however, porphyroblasts only occur in metabasites. The porphyroblasts in this study are all classified as syntectonic porphyroblasts, which form when the strain and growth rates in the host rock are the same. For determining shear sense with porphyroblasts, the asymmetry of the strain shadows and the rotation of the core are examined. Two types of porphyroblastic rotations are distinguished: oblique/sigmoidal-Si porphyroblasts and spiral-Si porphyroblasts. In oblique/sigmoidal-Si porphyroblasts the inclusions are either straight or slightly curved with an angle up to 90°, while in spiral-Si porphyroblasts the rotation exceeds 90°. Apart from being useful tools to determine shear sense, porphyroblasts may also provide a metamorphic history of their host rock, this can be done by looking at the inclusion minerals and their deformation and composition.

4.2.4 Mineral Fish

Mineral fish, or mica fish, are excellent shear sense indicators and have a strong preferred orientation. The composition of mineral fish can vary but the predominant mineral are Mica fish are split up from group 1-6 based on their shape after deformation, these subdivisions can be used to show what sense of shear the host rock underwent and the original orientation of the mica fish. Additionally, mica fish can be subject to truncation and its orientation aligning with C shear bands.

4.2.5 Shear Bands

Shear Bands are minor shear zones which form around older foliation due to extension. A distinction between two types of shear bands, C-type and C´-type is made. Being oblique to the shear zone and to the older foliation, the C´-type shear band is often found in strongly foliated micaceous mylonites and are usually short and wavy in their character. Due to the C´-type shear band being inclined to the shear zone, it is usually an effective method to ascertain a sense of shear in the host rock.

4.2.6 Boudinage

While not always a reliable shear sense indicator, boudinage can be used for just that purpose if it has an asymmetrically symmetry. The rigid slip movement and angular shape defines the domino boudinage. Shear sense can only reliably be determined if the boudin is parallel to the foliation as they may have the opposite geometry if oblique. Similarly, fractured porphyroclasts are also somewhat reliable shear sense indicators. Its mineral composition is often comprised of amphiboles, pyroxenes or feldspar grains and its sense of shear is best determined if fragmentation occurred in a shear zone, due to the more pronounced shearing forces.

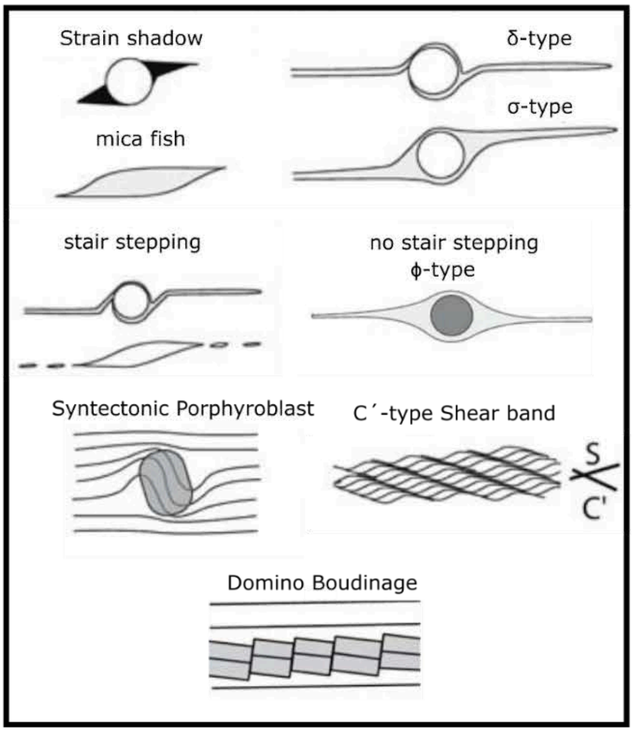

Figure 8: Illustration of various microstructures that will be featured in this study (examples include mica fish, different kinds of porphyroclast deformations, porphyroblast, shear bands and boudinage). The sense of shear is dextral, i.e., top-to-the-right.

5 Results and Interpretation

The mineral abbreviations used in this study follow a list of abbreviations published by Whitney & Evans (2010)(list of abbreviations A1). Full scan imagery of the samples that were not described in detail in the results are available in the Appendix B.

Metamorphic facies, composition, microstructure, and shear sense of each thin section were recorded and can be viewed in Table 1. Five of the samples are described below and are referred to as focused samples in the rest of the study.

Sample ID	Tectonic Unit	Protolith and facies	Minerals present	Microstructures	Shear Sense	Directional Shear Sense
Olympos-Ossa						
OL23/31 ★	Ampelakia Unit (CBU)	Metabasic blueschist	Chl, blue Amp, Qz, White Mica, Fsp, Ttn, Bt, Stp, Ep	medium grained matrix, fine grained tight foliations, folds, mica fish, porphyroclast	Dextral	Top-SW
OL23/35	Lower Pelagonian Zone	Metabasic greenschist	Qz, Dol/Cal, Fsp, White Mica, Chl, Act	medium grained foliation with Cal/Dol replacement, possibly shear bands and/or mica fish	Sinistral	Top-NE
OL23/37	Ampelakia Unit (CBU)	Metabasic greenschist	White Mica, Fsp, White Mica, Act	medium grained, folations with large spacing, porphyclast deformation	Sinistral	Top-SW
OL23/37c ★	Ampelakia Unit (CBU)	Metabasic blueschist	blue Amp, Chl, Fsp, Aug, Qz, Ttn, Ep	fine grained mylonitic foliation , porphyroclast deformation	Dextral	Top-S
OL23/43	Olympos-Ossa Unit	Metapelitic greenschist	Qz, Chl, White Mica, Bt	medium grained matrix, tight foliations, shear bands	Sinistral	Top-SW
OL23/47	Lower Pelagonian Zone	Metapelitic blueschist	Qz, White Mica, blue Amp, Chl, Bt	coarse grained matrix, fine grained spaced foliations, mica fish	Dextral	Top-SW
Pelion						
PE23/1 ★	Pelion Blueschist Unit	Metabasic blueschist	Chl, blue Amp, Qz, Cal, Fsp, Ttn, Ep	clear fine grained foliations , Cal/Dol replacement porphyroblast deformation, boudinage	Dextral	Top-SW
PE23/X1	Pelion Blueschist Unit	Metabasic greenschist	Chl, White Mica, Qz, Fsp, Ttn, Bt	medium grained matrix, alternating mylonitic foliations, porphyroclast deformation	Dextral	Top-SW
PE23/X2 ★	Pelion Blueschist Unit	Metabasic blueschist	Chl, Qz, Ep, Act , White Mica, Fsp, blue Amp	coarse grained matrix, clear foliations with inclusions of Ep, shear bands, porhyroblasts	Dextral	Top-NE
PE23/X3	Pelion Blueschist Unit	Metabasic greenschist	Chl , Qz, Fsp, White Mica, Cal/Dol, Ttn	fine grained mylonitic foliations, porphyroclast deformation, boudinage	Sinistral	Top-NE
PE23/51	Eohellenic Nappe	Metabasic greenschist	Chl, Act, Qz, Fsp, Ep	fine grained mylonitic foliation, sigmoid & porphyroclast deformation	Sinistral	Top-SW
PE23/54	Pelion Blueschist Unit	Metabasic greenschist	Tr, Act, Chl, Qz, Fsp	fine grained, spaced foliations, shear bands	Sinistral	Top-NE
PE23/55	Pelion Blueschist Unit	Metabasic greenschist	Qz, Ep, Chl, Opq, Ttn, Act	fine grained, tight foliations, veins	Dextral	Top-NE
PE23/56	Pelion Blueschist Unit	Metabasic greenschist	Qz. Chl, Fsp, White Mica, Ep, Act	very fine grained mylonitic foliations, porphyroclast deformation	Dextral	Top-SW
PE23/57	Pelion Blueschist Unit	Metabasic greenschist	Qz, Dol/Cal, Qz, Chl, Act, Fsp	coarse grained matrix, fine grained clear foliations, Cal/Dol replacement, shear bands	Dextral	Top-NE
PE23/58	Pelion Blueschist Unit	Metabasic greenschist	Chl, Act, Qz, Cal/Dol, Ep, Tr, Fsp	coarse grained matrix, fine grained clear foliations, Cal/Dol replacement, shear bands	Dextral	Top-NE
Skiathos						
SK23/60	Upper Pelagonian Zone	Metabasic greenschist	Qz, Cal/ Dol, Chl, Bt, White Mica	fine grained mylonitic foliation, mica fish	Sinistral	Top-NE
SK23/61 ★	Upper Pelagonian Zone	Metabasic greenschist	White Mica, Qz, Cal, Dol, Ep, Chl, Act, Hbl, Fsp	fine grained foliations in a large grained matrix, porphyroclast deformation, mica fish	Sinistral	Top-SW
SK23/62	Upper Pelagonian Zone	Metabasic greenschist	Dol/Cal, Qz, White Mica, Fsp, Act	very coarse grained, fine grained foliation obliterated by porphyroclasts, mica fish	Dextral	Top-SW

Table 1: Geological characteristics of rock samples from the Olympos-Ossa, Pelion, and Skiathos regions. The table includes data on tectonic units, protoliths and facies, minerals present, microstructures, shear sense, and directional shear sense. The red stars highlight the focused samples that are presented in the results

5.1 Olympos-Ossa

5.1.1 OL23/31

Sample OL23/31 classified as metabasic blueschist (Fig. 9 a), contained Wm, blue Amp, Chl, Fsp, Ep, Ttn, Bt and/or Stp (Evans, 1990). This is expected from the CBU as the unit has undergone high P metamorphism (Schermer et al., 1990). The possible Stp growth is observed growing over quartz along rims, the formation of Stp could indicate a Fe-rich Chl and Bt (Magyarosi et al., 2002), which further indicates its metabasic protolith. Notably this sample had the most varied minerals out of the total samples in its main foliation namely blue Amp, Wm, Chl and Bt (Fig. 9 b). The blue Amp is mainly found in abundance in the foliations mostly appearing as characteristic amphibole needles (Fig. 9 e, g). However, Mineral replacement of the blue Amp by Bt as well as chloritization is seen throughout the thin section, hinting that the sample is a retrograde blueschist. Furthermore, Chl undergoing alteration with Bt was also observed (Fig. 9 e, f). This is likely due do the sample having a high water content and a further sign of retrograde metamorphism (Eggleton and Banfield, 1985; Kogure and Banfield, 2000).

Structurally the foliation was fine grained and distinct with the microlithons containing Qz and Fsp (Fig. 9 a). Notably the entire sample had two large folds which altered the grain alignment around the folding structures (Fig. 9a). The general shear sense was dextral, this was identified through large grainy group 1 mica fish (Fig. 9 d). Another indicator present was deformed porphyroclasts which were composed of Fsp, additionally a single Ep porphyroclast was observed. The Fsp porphyroclasts identified as σ-type and had strains caps which corresponded with the minerals in the surrounding foliations, the strain shadows would either be entirely made of Qz or partially Qz on one side of the clast, with the other side exhibiting the same minerals as the foliation. The Ep porphyroclast had fractures and exhibited δ-type dextral deformation without stair stepping and had a Wm reaction rim (Fig. 9 c). Dextral shear sense was also visible in a set of blue Amp needles C´ shear bands (Fig. 9 g). A top-SW directional shear sense was determined through the dextral movement towards top-SW.

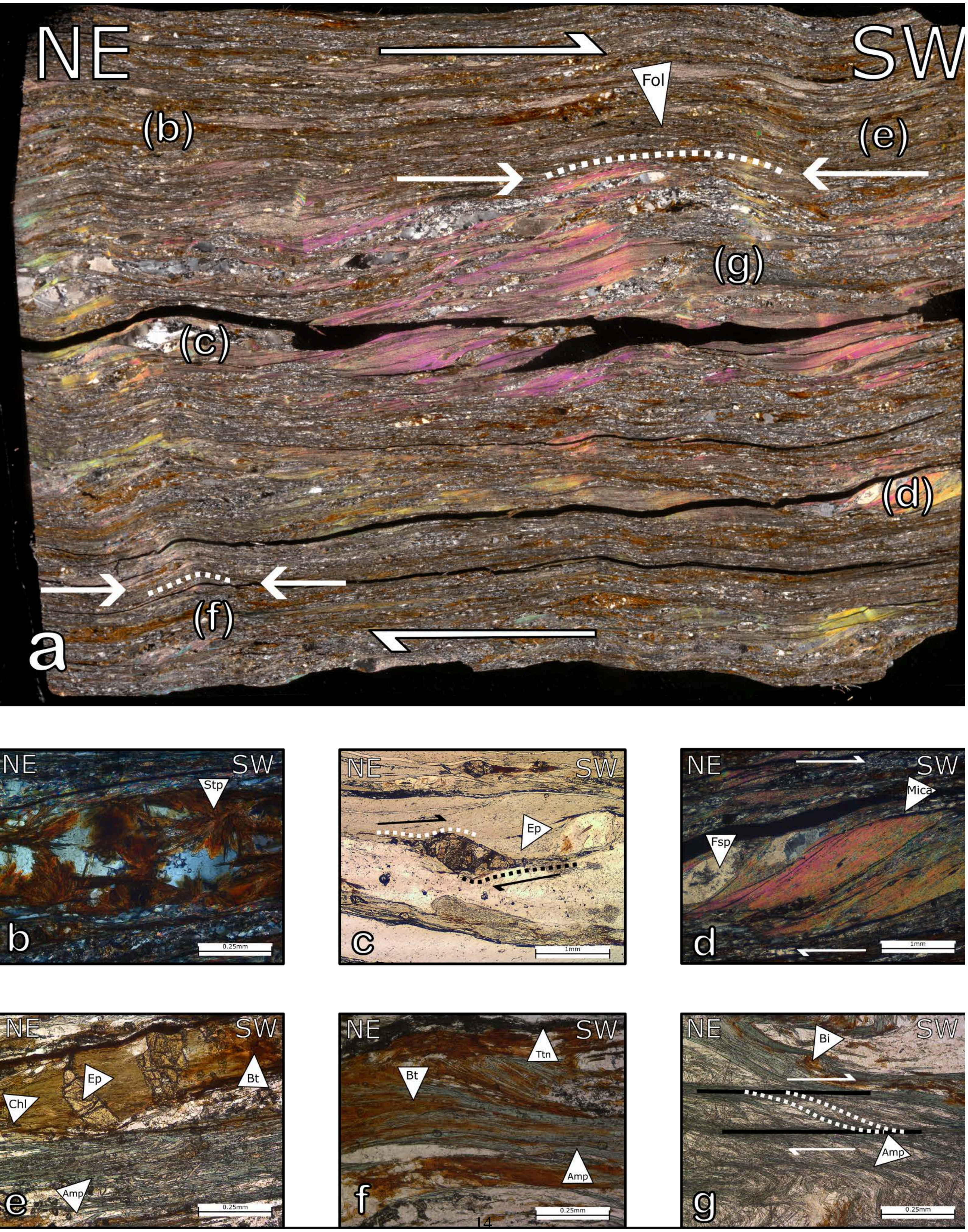

NE
SW
Fol
(b)
(e)
(g)
(c)
(d)
(f)
a
NE
SW
Stp
b
0.25mm
NE
SW
Ep
c
1mm
NE
SW
Mica
Fsp
d
1mm
NE
SW
Ep
Bt
Chl
Amp
e
0.25mm
NE
SW
Ttn
Bt
Amp
f
0.25mm
NE
SW
Bi
Amp
g
0.25mm

Figure 9: Photomicrographs of sample OL23/31 showing a dextral movement towards SW. (a) A fullscan of the sample showing the folds, and the location of the photomicrographs (XPL). (b) Possible Stp growth over Qtz (XPL). (c) A dextrally deformed Ep δ-type porphyroclast with shearing arrows (PPL). (d) Deformed mica fish showing dextral movement (XPL). (e) Mineral alteration of blue Amp with both Chl and Bt, while Chl is being altered by reactions with Bt (PPL). (f) Blue Amp being altered by Bt, with a rim of Ttn on the top (PPL). (g) Dextral movement of blue Amp showcased by C′ shear band (PPL).

5.1.2 OL23/37c

Sample OL23/37c exhibited a blueschist-facies mineral composition of Chl, blue Amp, Fsp, Aug, Qz, Ttn and Ep (Fig. 10a). With the presence of the relict Aug minerals setting its mafic origin(Fig. 10e) (Messiga et al., 1995). The main foliation included Wm, Ttn and blue Amp, the foliation was identified as a fine grained mylonitic foliation with variating width between the individual foliations, with the microlithons composed of Qz and Blue Amphibole. Blue Amp needles were observed in the microlithons (Fig. 10c) and some of the minor foliations and showed signs of the blue Amp undergoing mineral replacement. Along with the blue Amp rich foliations signs of very small Chl grains are seen hinting at blueschist retrogression (Fig. 10c).

The main structure of sample OL23/37c, are porphyroclasts indicating a general dextral movement (Fig. 10b). The porphyroclasts in the thin section were comprised of either Fsp or fractured Aug many of which exhibited simple twinning (Fig. 10e). Observations classified the porphyroclasts as ϕ- and σ-type porphyroclasts with strain shadows, its strain caps having the same composition as the main foliations (Wm and Ttn). The strain shadows predominantly consisted of the foliation mineral composition, while a few of the porphyroclasts exhibited small Qz strain shadows (Fig. 10b). Notably, the strain caps of one porphyroclast were replaced by blue Amp (Fig. 10d). The dextral movement was then concluded to be directionally shearing toward top-SW

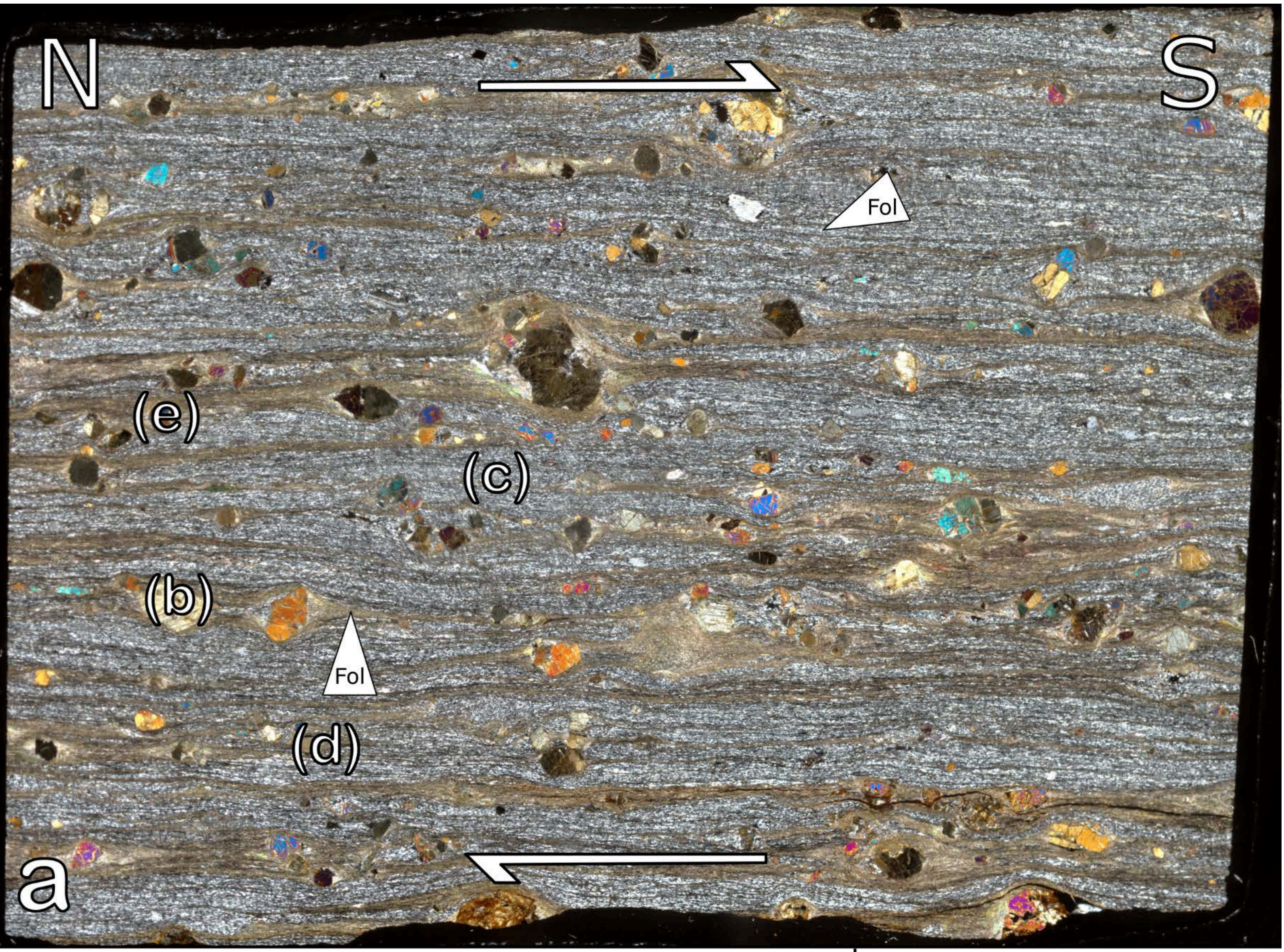

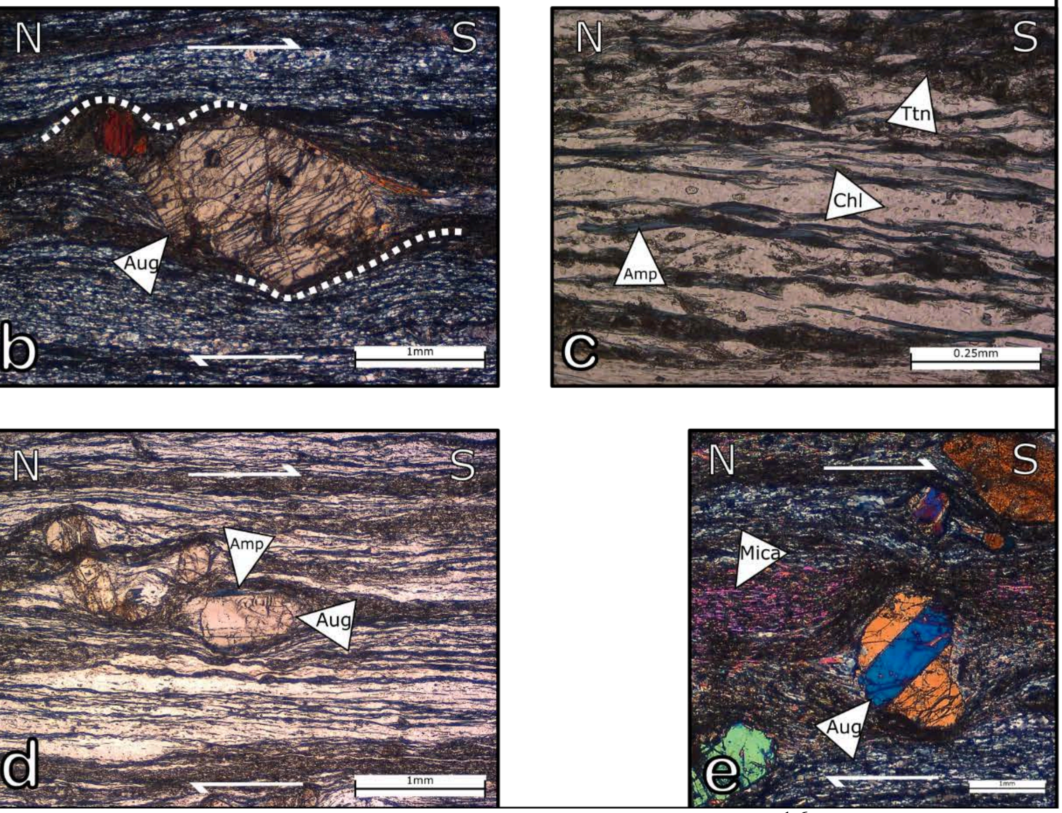

Figure 10: Photomicrographs of sample OL23/37c showing a dextral movement towards S. (a) A fullscan of the location of the photomicrographs (XPL). (b) An angled Aug deformed porphyroclasts in a dextral direction (XPL), its strain shadow being filled with Qtz. (c) Close-up picture of the blue Amp rich foliation, with very small Chl crystals between the blue Amp needles (PPL). (d) Deformed porphyroblasts where its strain caps have been altered with blue Amp (PPL). (e) Typical simple twinning of Aug porphyroclasts being deformed by the main foliation (XPL).

5.2 Pelion

5.2.1 PE23/1

Sample PE23/1 classified as a metabasic blueschist (Fig. 11a), showed a high P/T metamorphism through its mineralogical composition (Winter, 2014). It was notably one of two samples exhibiting the presence of porphyroblasts. The fine-grained foliations were distinct throughout the thin section and were predominantly composed of Chl and blue Amp, while the rest of the thin section included Qz, Cal, Ms, Dol, Fsp and Ttn, as well as Opq minerals. Chloritization was common throughout the thin section where Chl was replacing the blue Amp in the shear zones indicating at retrograde metamorphism (Fig. 11b) (Bucher and Grapes, 2011). A large shear zone was present where the blue Amp with inclusions of Opq minerals had not under as much chloritization (Fig. 11d).

The metamorphic structures in the thin section were mainly dominated by porphyroblast deformations, along with microboudinage. The porphyroblasts were classified as syntectonic porphyroblasts with sigmoidal S_i pattern of which one indicated sinistral movement (Fig. 11e), while the rest of the porphyroblasts indicated dextral movement (Fig. 11c, f). The inclusion minerals in the porphyroblasts were made of blue Amp, throughout the entire sample. The microboudinage composed of Fsp porphyroblasts with dextral rotation, additionally the boudinage was foliation oblique from bottom left to top right, which further indicated a dextral shear sense (Fig. 11g). The strain shadows were either composed of the same mineral composition as the foliations or filled in with Qz and/or Dol/Cal (Fig. 11c, f). The Dextral shear sense outweighed the singular sinistral porphyroblast, and then a top-SW directional shear sense could be concluded.

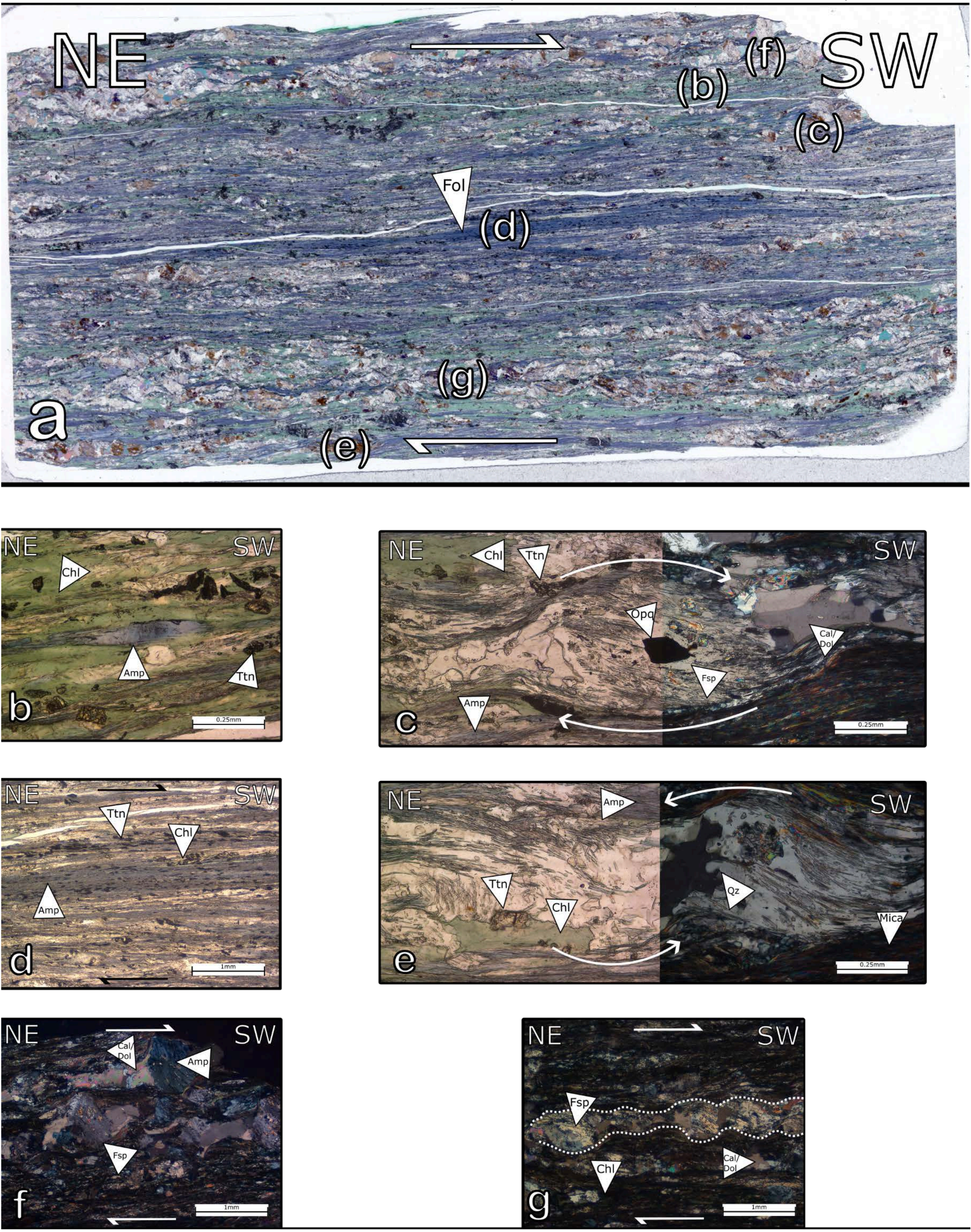
NE
SW
(b)
(f)
(c)
Fol
(d)
(g)
(e)
a
NE
SW
Chl
Amp
Ttn
b
0.25mm
NE
SW
Chl
Ttn
Opq
Cal/Dol
Fsp
Amp
c
0.25mm
NE
SW
Ttn
Chl
Amp
d
1mm
NE
SW
Amp
Ttn
Chl
Qz
Mica
e
0.25mm
NE
SW
Cal/Dol
Amp
Fsp
f
1mm
NE
SW
Fsp
Chl
Cal/Dol
g
1mm

Figure 11: Photomicrographs of sample PE23/1 showing a dextral movement towards SW. (a) A fullscan of the location of the photomicrographs (PPL). (b) Blue Amp being altered into Chl, accompanied by the presence of Ttn (PPL). (c) A syntectonic sigmoidal S_i pattern Fsp porphyroblast, with dextral rotational movement and blue Amp inclusions. A large Opq mineral is also visible in the centre and Cal/Dol growth in the strain shadows (PPL left, XPL right). (d) Foliation with predominantly blue Amp with a lot of Ttn inclusions (PPL). (e) The single sinistral rotating syntectonic porphyroblast with traces of a sigmoidal S_i pattern the original porphyroblast mineral has been altered and then replaced by Qz (PPL left, XPL right). (f) Further examples of dextral rotational Fsp porphyroblasts with Cal/Dol growth in the strain shadows (XPL). (g) Boudinage which is slightly oblique to the foliation hinting at dextral shearing (XPL).

5.2.2 PE23/X2

Sample PE23/X2, classified as a metabasic retrograde blueschist (Fig. 12a)(Ernst, 1988), consisted of a mineral assemblage of Wm, Qz, Ep, Chl, Fsp and blue Amp. The main foliation in this sample included Wm, Chl, and blue Amp was identified in minor foliations (Fig. 12b), additionally being the mineral found in the porphyroblasts throughout the thin section (Fig. 12c). The blue Amp in this sample is unstable as it had been reacting with Chl, there were however some areas where the blue Amp had undergone less Chl alterations.

The distinct foliations with inclusions of Ep in a medium grained matrix, had shear bands as the main shear sense indicator. The C´-type shear bands were mainly exhibiting dextral movement (Fig. 12d), with one single shear band indicating sinistral movement. Furthermore, the shear band minerals were made of the same minerals that made up the main foliation. Syn-tectonic sigmoidal S_i pattern porphyroblasts were present in the sample, the inclusion mineral in the porphyroblasts were composed of blue Amp, appearing above Qz likely through a mafic mineral alteration followed by Qz growth (Fig. 12c). It could be argued that these are not a porphyroblast, but rather just dextral deformation because of the absence of the original enclosing mineral (Vernon, 1986). The general dextral movement throughout the sample concluded that this sample had a top-NE directional shear sense.

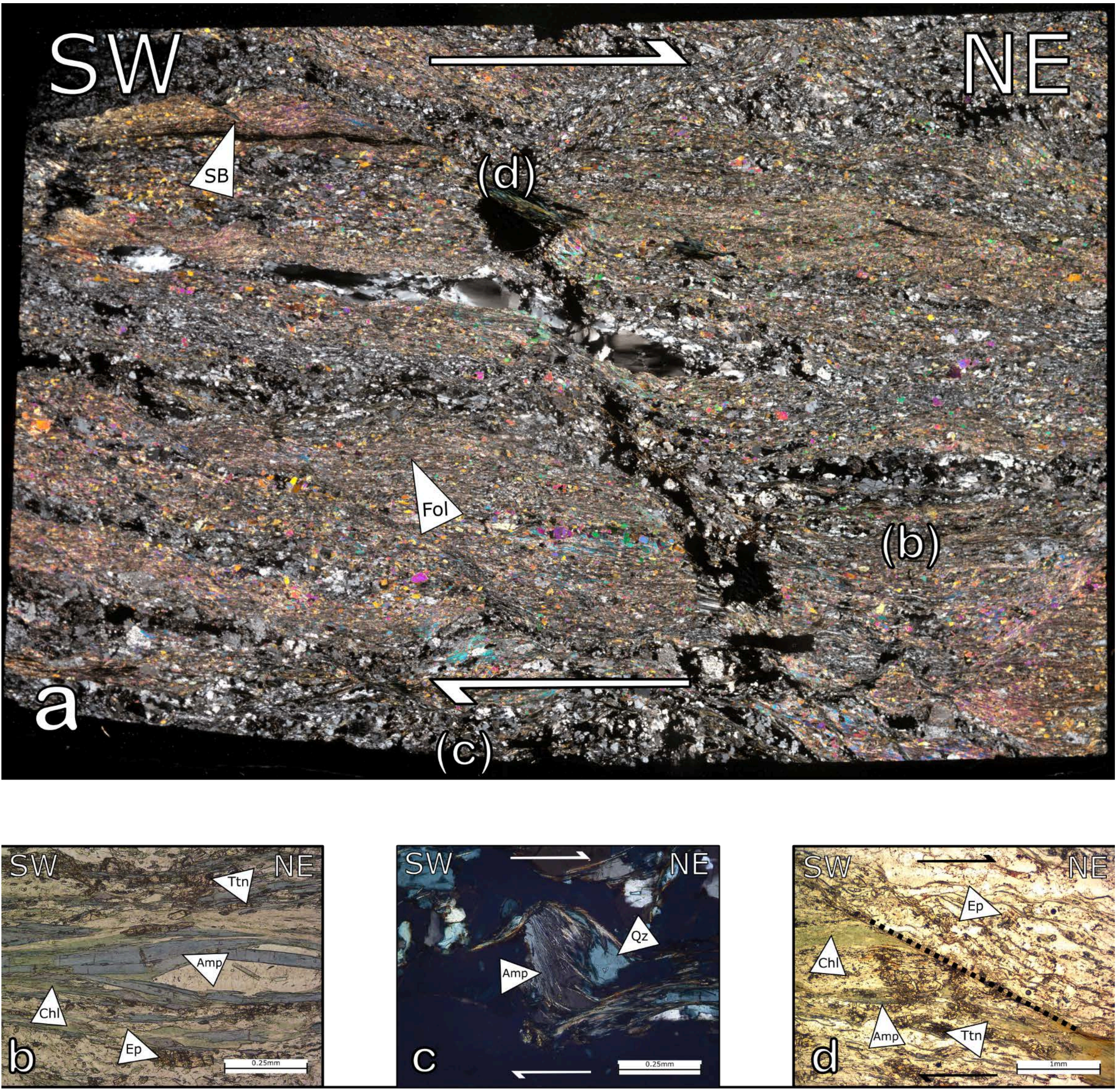

Figure 12: Photomicrographs of sample PE23/X2 showing a dextral movement towards NE. (a) A fullscan of the location of the photomicrographs (XPL). (b) Blue Amp being altered by Chl and accompanied by small Ttn crystals and Ep (PPL). (c) A Qz syntectonic sigmoidal S_i pattern porphyroblast shows blue Amp inclusions with dextral rotational movement (XPL). (d) Dextral shear band composed of Chl with small needles of blue Amp being visible alongside Ttn and Ep (PPL).

5.3 Skiathos

5.3.1 SK23/61

Sample SK23/61 classified as a metabasic greenschist (Fig. 13 a), with a mineral assemblage consisting of Wm, Qz, Cal, Dol, Ep, Chl, Act, Tr, Fsp, Opq and notably the only sample containing Hbl (Fig. 13b), further indicating its mafic origin. The Hbl indicates that this sample underwent upper greenschist or retrograde amphibolite-facies metamorphism (Harte and Graham, 1975). Apart from the higher P/T minerals found, the sample also exhibits low metamorphism as Cal and Dol are present, likely formed in tandem with Chl, Ep, Hbl and Fsp as the mineral composition is so varied and as metabasic NCaFMASCH pseudosection calculations show stable paths the mineral composition has a stable zone(Elmer et al., 2006).

The SK23/61 sample included Wm rich fine grained space foliations, with Qz rich microlithons. Sinistral movement was indicated through deformed porphyroclasts, microboudinage and mica fish (Fig. 13c). The porphyroclasts comprised of Fsp (Fig. 13e), had undergone partial replacement through sericitization or Dol/Cal replacement. The porphyroclasts were identified as σ-type porphyroclasts with Qz strain shadows and foliation strain caps, with minimal stair-stepping. One set of Fsp domino boudins (Fig. 13d) was also indicating sinistral movement, with Qz and Wm filling in the gaps of the separated boudins. The sample shears towards top-SW with its sinistral movement

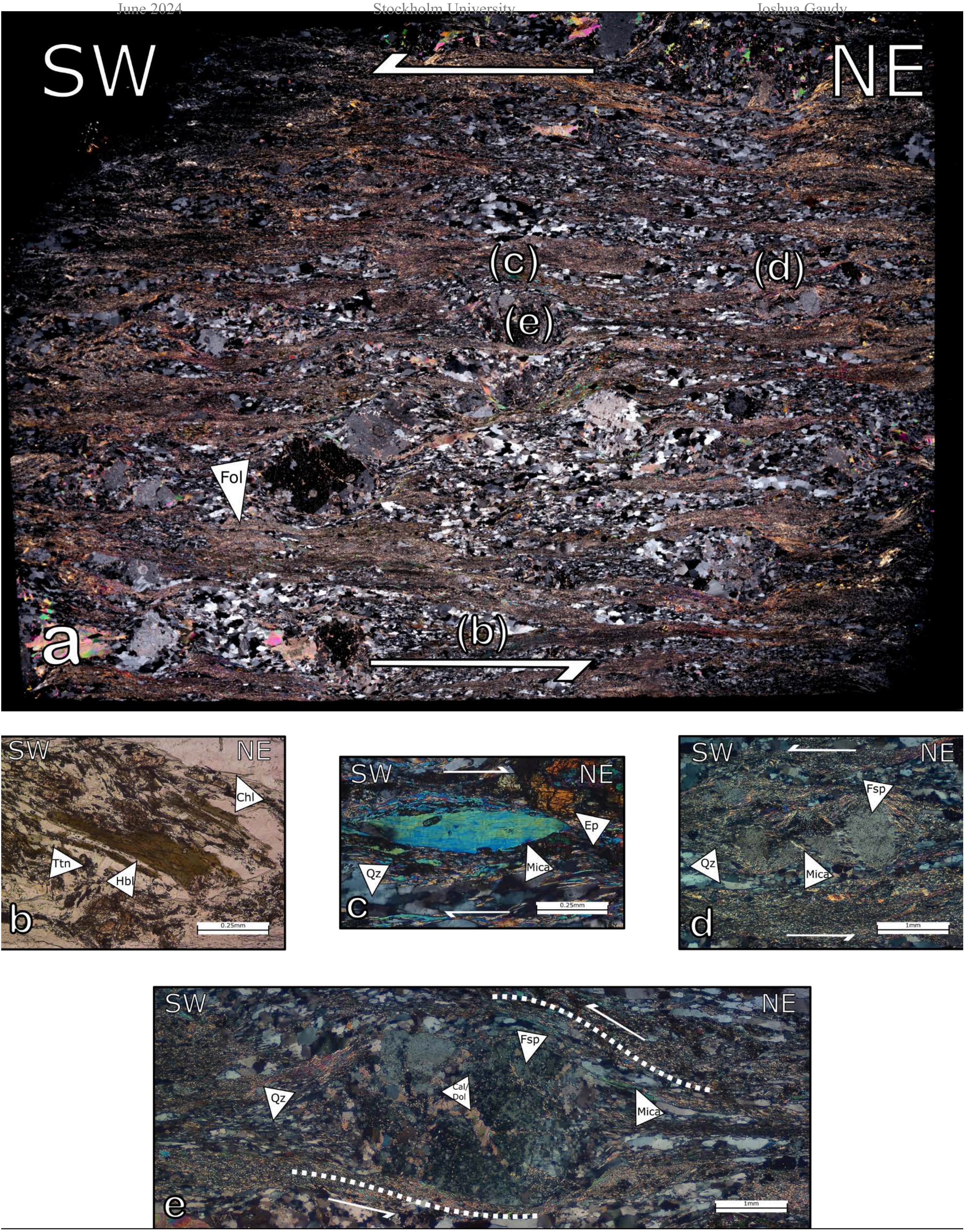
SW
NE
(c)
(d)
(e)
Fol
(b)
a
SW
NE
Chl
Ttn
Hbl
0.25mm
b
SW
NE
Ep
Qz
Mica
0.25mm
c
SW
NE
Fsp
Qz
Mica
1mm
d
SW
NE
Fsp
Qz
Cal/
Dol
Mica
1mm
e

Figure 13: Photomicrographs of sample SK23/61 showing a dextral movement towards SW. (a) A fullscan of the location of the photomicrographs (XPL). (b) Relict Hbl mineral being replaced by greenschist-facies minerals like Chl (PPL). (c) Mica fish indicating dextral movement (XPL). (d) Dextral deformation of Fsp domino boudinage with Wm growth in-between the boudins (XPL). (e) Deformed and fractured Fsp porphyroclast with Qz strain shadows which have foliation inclusions. Strain caps are made up of the foliation material, and fractures are filled with Cal/Dol (XPL).

6 Discussion

The study aimed to analyse the 19 thin sections collected from NE Greece in the Olympos-Ossa, Pelion and Skiathos regions, to identify the mineral assemblages, microstructures and shear sense. The data are summarized in Table 1. Here we discuss the potential meaning of the data for tectonic evolution of the regions in the Aegean Sea region.

6.1 Olympos-Ossa

In the 6 samples from the Olympos-Ossa region three were collected from the Ampelakia Unit (CBU) which stated before is a part of the CBU, two from the Lower Pelagonian Unit and one from the Tripolitza unit (Godfriaux, 1968; Kilias, 2024). The general directional shear sense of five of the samples were top-SW or top-S, while OL23/35 was shearing towards top-NE (Fig. 3). However, the shear sense of OL23/35 was indicated to be dextral towards top-NE, but a sinistral shear sense top-SW could be argued, as the shear sense indicators were very few and hard to discern. The general shear direction of the samples is top-SW which aligns with studies made on the same metamorphic facies and the same region (Schermer, 1993; Schermer et al., 1990; Walcott, 1998). With the general shear sense of the samples collected from Olympos-Ossa region are shearing towards top-SW. Combined with the mineral composition and the metamorphic facies, it would be safe to assume that the thrusting is equivalent to the high P blueschist and greenschist-facies metamorphism. This metamorphism occurs at 6-8 kbar and 200-350 °C (Kilias, 2024; Schermer, 1990), which is assumed to have occurred between 64-36 Ma (Schermer et al., 1990; Walcott, 1998). The metamorphic event occurred as the CBU experienced ductile shearing against the underlying Tripolitza Unit in a downward and top-SW direction (Lips et al., 1998; Schermer, 1993) and will be further discussed in *Sec 6.2* (Fig. 14).

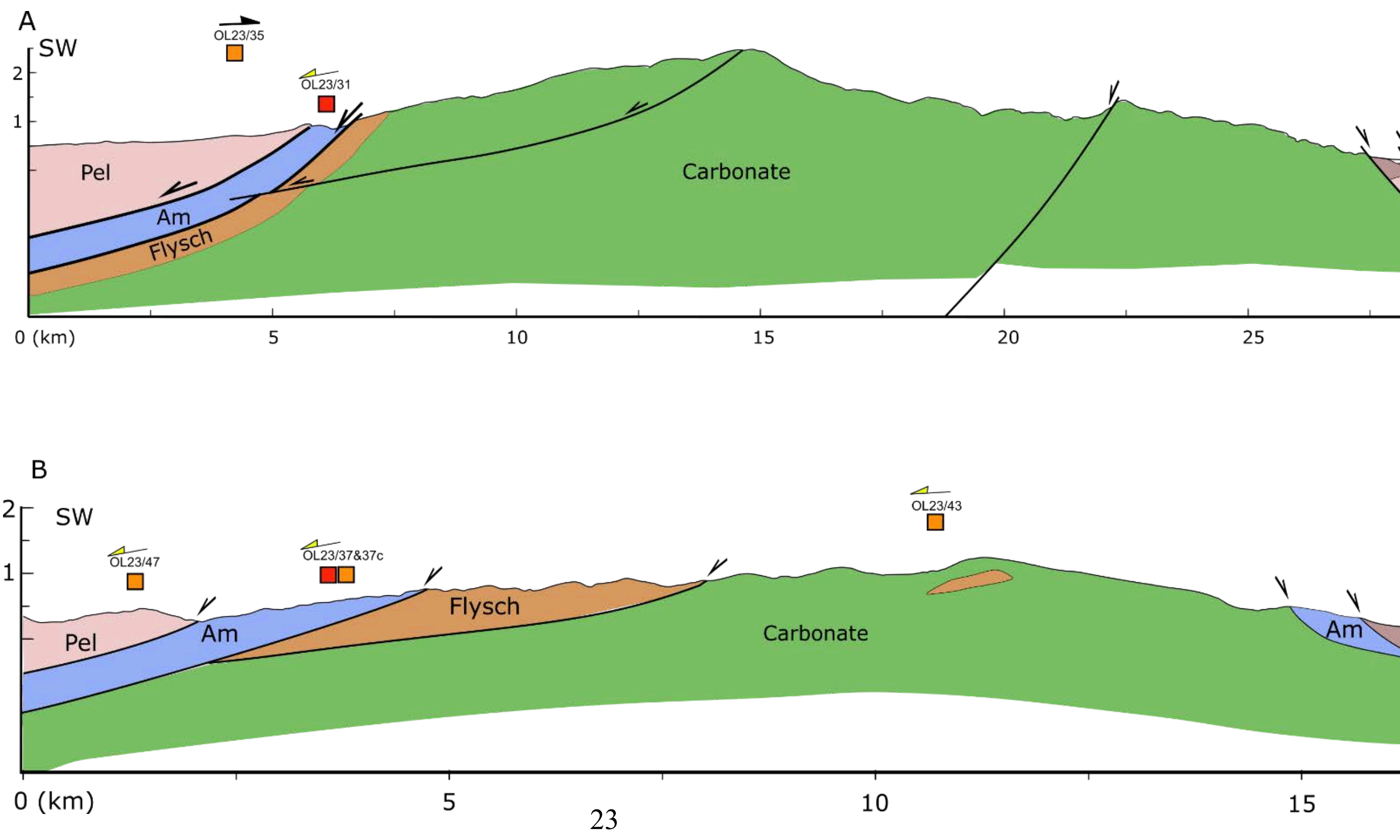

Figure 14: Two cross-sections (see figure 4 for unit description). The filled in arrows showcase the directional shear sense, either top-SW (Yellow) or top-NW (Black). Orange filled boxes show the rough sample location along with its Sample ID, the boxes highlighted in red show the "focused" samples. For A-A′ one is shearing top-SW while the other on is shearing in the opposite direction. Notably the black arrow is above the yellow to indicate an order of time with the bottom shear being older than the overlying arrow. B-B′ only exhibits top-SW shear sense.

6.2 Pelion

Out of the 10 samples from the Pelion regions 9 of them were collected from the PBU, while the last sample was from the Eohellenic Nappe (Fig. 3). Out of the 10 total samples 8 of them were metabasic greenschist-facies rocks, while the other two were classified as metabasic blueschists. The two blueschist samples from the Pelion region shows opposite directional shear sense. Where sample PE23/1 shearing top to the SW, PE23/X2 exhibits a top-NE directional shear sense. The top-SW shear sense from PE23/1 is consistent with the high-P metamorphic event with approximate P/T at 8 kbar and 350 to 400 °C (Lips et al., 1999). The timing of this metamorphic event ranges from 57 to 53 Ma (Hinshaw et al., 2023), however, preliminary dating by Hong et al. set the metamorphic event at 53 to 45 Ma. Sample PE23/X2 on the other hand, exhibited a top-NE shear sense had undergone retrograde metamorphism determined by the chloritization of Blue Amp. With the determination of its retrograde nature, it could be argued that the top-NE shear sense is correct as retrograde blueschist in the Pelion region are usually varied and can shear top-SW as well as top-NE(Walcott, 1998). Of the 7 greenschist and sub-greenschist-facies samples in the PBU, 5 of them are shearing towards top to the NE, which could coincides with a greenschist overprint over the underlying PBU (Kilias et al., 1995; Lips et al., 1999; Walcott, 1998). The greenschist overprint may have occurred from 37 to 16 Ma (Lips et al., 1999), while another ongoing study has dated this top-NE shearing at 22-15 Ma (Hong et al., unpublished data). This could be interpreted to be related to the Miocene extension, which started at 23 Ma (Ring et al., 2010) and the low angle fault of the Pelagonian Unit and Eohellenic Nappe over the CBU.

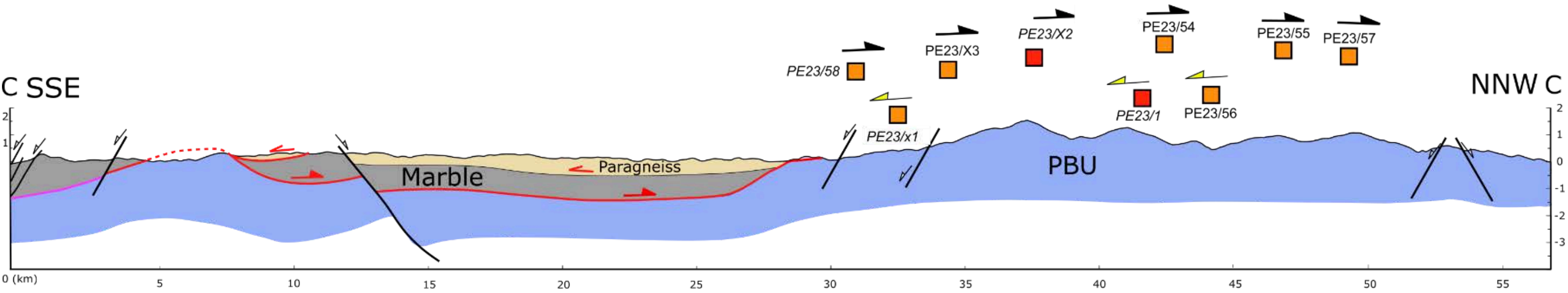

Figure 14: Cross-section C-C′ (see Figure 5 for unit description). The filled in arrows showcase the directional shear sense, either top-SW (Yellow) or top-NW (Black). Orange filled boxes show the rough sample location along with its Sample ID, the boxes highlighted in red show the "focused" samples. 3 top-SW shearing samples highlighted in yellow arrows and 6 shearing top to the NE, indicated with black arrows. Notably the black arrows are above the yellow to indicate an order of time with the bottom shears being older than the overlying arrows.

6.3 Skiathos

The three samples collected from the Skiathos Island were sampled from the Upper Pelagonian Unit (Fig. 3), which is the predominant tectonic unit on Skiathos (Ferentinos, 1973). More specifically, SK23/60 and SK23/61 were obtained from a border between the Upper Cretaceous Carbonates and Upper Cretaceous-Paleogene flysch, while sample SK23/62 belongs to the Upper Cretaceous Carbonates. The mineral composition of these samples does not differ much and contain common greenschist-facies minerals, which is consistent with the greenschist-facies metamorphism of the Upper Pelagonian Unit (Schermer et al., 1990; Yarwood and Dixon, 1977). Similarly the minerals that make of the main foliations in the thin sections include in all cases Wm with the absence of Chl in

SK23/61, which aligns with the studies conducted on the adjacent Skopelos Island (Porkoláb et al., 2019).

When observing the general shear sense of the three samples, it's noted that the shear sense for sample SK23/60 & SK23/61 are sinistral, while SK23/62 has a dextral shear sense. However, the directional shear sense of SK23/60 shows top-NE, where the SK23/61 & SK23/62 indicate top-SW, which results in SK23/60 & SK23/61 exhibiting both a top-SW and top-NE shear sense. Furthermore, the top-SW shear sense samples may have been sheared during the same time period 55-60 Ma, while the top-NE shearing, which followed the top-SW shearing was dated at 30-35-Ma (Porkoláb et al., 2019, 2020). This could additionally explain the top-SW and top-NE shearing at SK23/60 & SK23/61 where the older top-SW shear sense possibly apart of the Upper Cretaceous Carbonates, while the overlaying top-NE shearing unit would belong to the Upper Cretaceous-Paleogene flysch, which is evident in the D-D′ cross-section and in their structural differences.

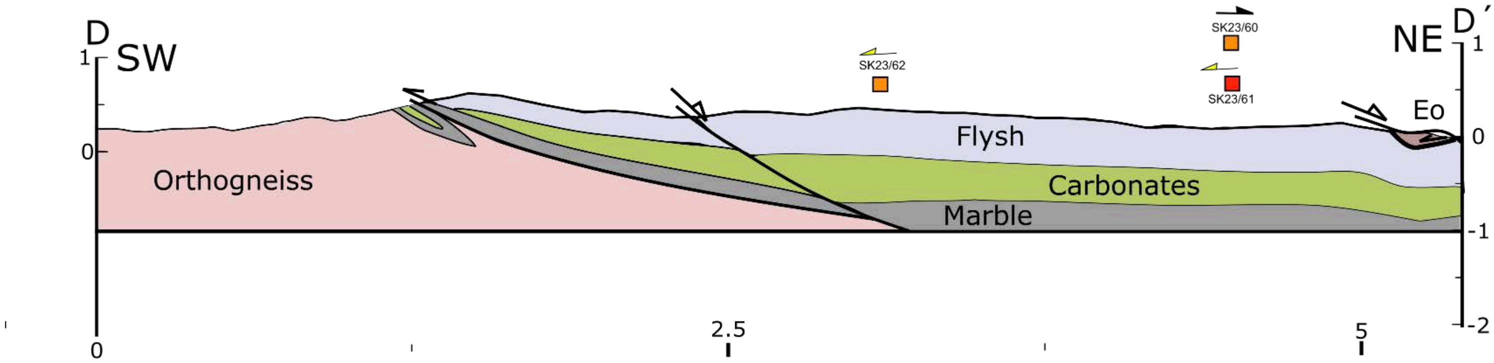

Figure 15: Cross-section D-D′ (see Figure 5 for unit description). The filled in arrows showcase the directional shear sense, either top-SW (Yellow) or top-NW (Black). Orange filled boxes show the rough sample location along with its Sample ID, the boxes highlighted in red show the "focused" samples. Notably the black arrow is above the yellow ones to indicate an order of time with the bottom shears being older than the overlying arrow.

The Upper Pelagonian and Eohellenic Nappe, which are now exposed on Skiathos, were tectonically stripped off from Pelion (Jacobshagen and Wallbrecher, 1984). The shearing and greenschist-facies conditions that occurred on Skiathos, likely reflect the deformational and metamorphic history of the units before their removal.

6.4 Tectonic history of CBU/PBU

First looking at the tectonic history of the CBU in the Olympos-Ossa region, which starts with the subduction the units in following order Eohellenic Nappe, the Pelagonian Unit, Ampelakia and the Tripolitza Unit (Jacobshagen and Wallbrecher, 1984; Kilias, 2024). Following the subduction of the Tripolitza a top-SW blueschist and greenschist-facies shear occurred along the contact between the Ampelakia and the Tripolitza units (Fig. 16a). Since this movement also affects the late Eocene Ossa flysch of the Tripolitza unit, its probable age ranges from the Eocene to the Oligocene (~30-40 Ma (Schermer et al., 1990)). The shearing is associated with the omission of the middle- and lower-CBU, as the thrusting in the subduction zone during and after accretion of the units during high-pressure metamorphism would lead to an intact tectonometamorphic sequence (Lips et al., 1999; Schermer et al., 1990; Walcott, 1998). Omission of the middle- and lower-CBU, were caused by out-of-sequence thrusting (where newer faults cut across and override older ones), which cuts own into the tectonic sequence during thrusting. Leading to the upper-CBU being overthrust onto the Tripolitza unit (Fig. 16b). Exhumation of the Tripolitza unit occurred in the region during the Oligocene to the Miocene (Kilias, 2024), where the exhumation caused the overlying units were thrust to each side of the Tripolitza unit (Fig. 16c). From here the Olympos region and Ossa region vary as seen in cross-section A-A´ and B-B´ (Fig. 14). On the NE side of A-A´ a set of high angle normal faults are found, where the Eohellenic nappe is overlain by quaternary deposits. These faults were likely caused by the perpendicular North Anatolian Fault causing external stress in the region (Fig. 1a). While on the B-B´ cross-section the Eohellenic unit cuts out the underlying units possibly due to another out of sequence thrust or through similar normal faulting as in cross-section A-A´.

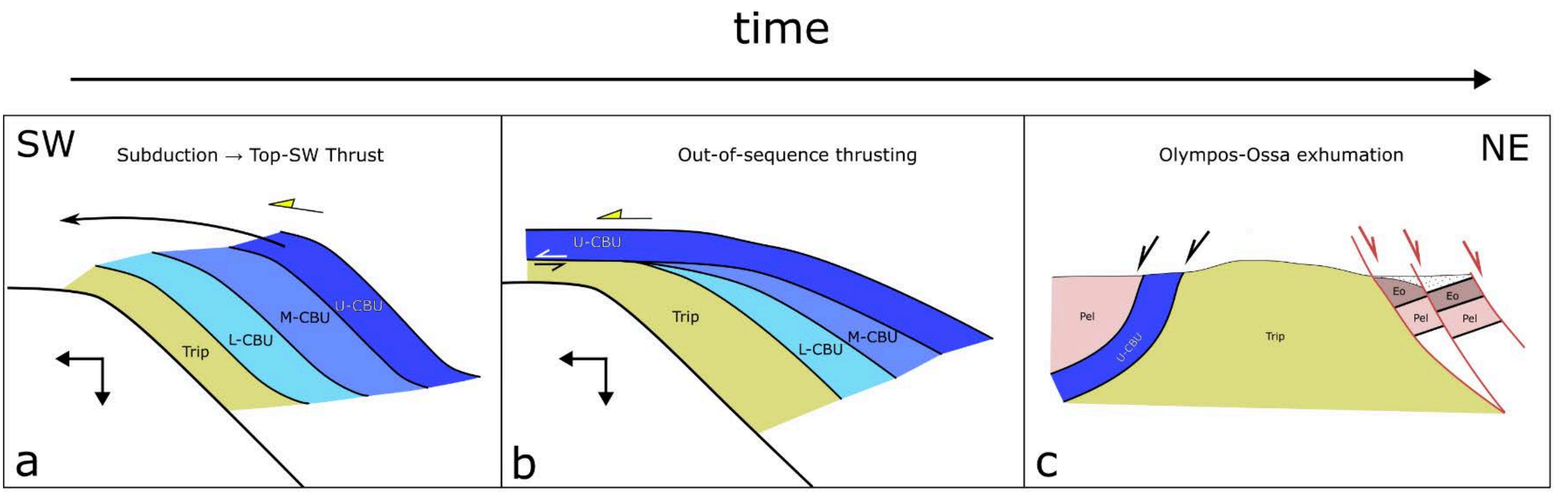

Figure 16: Illustrations of the tectonic history of the CBU in the Olympos-Ossa region. (a) Shows the stacking of the units above the subduction zone and the initial top-SW thrust affecting the Upper-CBU. (b) As the top-SW progresses the Middle- and Lower-CBU gets cut out and the upper-CBU overprints the Tripolitza Unit. (c) Illustrates the tectonic events of the Olympos region. Following the overprint the Tripolitza Unit gets exhumed and deform the surrounding units to be thrust to each side of the Tripolitza. The red arrows show the large high angle faults likely caused by the perpendicular stresses of the North Anatolian faults.

The Pelion region follows a similar SW-NE tectonic history as the Olympos-Ossa region. However, unlike the Olympos-Ossa region, the Pelion region only exhibits the Eohellenic Nappe, Pelagonian Unit and the CBU, and does not include the exhumation of the Tripolitza Unit is local to the Olympos-Ossa region and Kranea (Fig. 1a)(Godfriaux, 1968; Kilias et al., 1991). Furthermore, the Upper-PBU is absent, while the middle-PBU is present and the lower-PBU likely remains underneath the Middle-PBU. The omission of the Upper-PBU likely occurred after the blueschist-facies metamorphic conditions, as both the Eohellenic Nappe and the Upper Pelagonian Unit overprinted the under lying PBU. A probable cause for this overprint is the aforementioned Miocene lithospheric extension, which was an ongoing event in the Aegean Sea region (Jolivet et al., 1994). This would have caused a top-NE shearing greenschist and sub-greenschist overprint at 22-15 Ma (Hong et al., unpublished data). Extensional faulting would also provide an explanation for the absence of the Lower Pelagonian Unit in large parts of the tectonosection (Fig. 17).

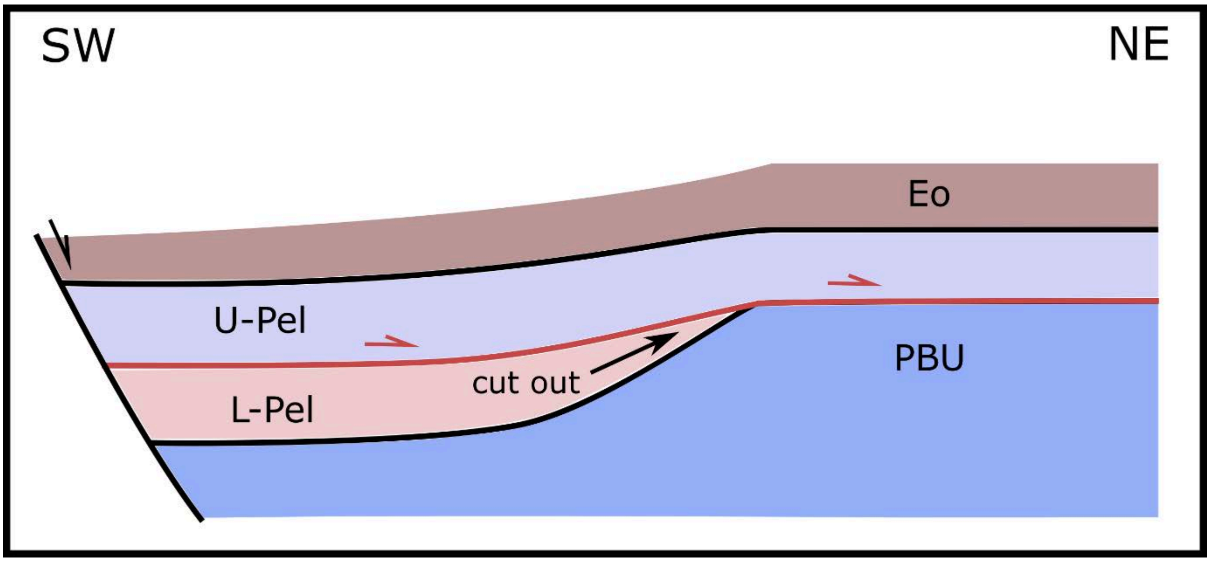

Figure 17: Illustration showing extensional faulting in the Pelion region cutting out the Lower Pelagonian Unit, as the Upper Pelagonian and Eohellenic Nappe overprinting the PBU.

When looking at a P-T path tectono-metamorphic path and exhumation path of the Paleocene-Eocene blueschist belt in the Olympos-Ossa region (Altherr et al., 1982; Kilias, 1995; Schermer et al., 1990) and the Pelion Peninsula (Lips et al., 1999, 1998; Schermer et al., 1990)(Fig. 7). It becomes apparent that the paths are very similar to each other and could have undergone the similar metamorphic conditions and tectonic movements. Comparing top-SW shearing samples from the Olympos-Ossa region and the top-SW directional shear sense from the Pelion region, as well as the timing of the metamorphic events. We find that PE23/1 has experienced similar metamorphic conditions to the Ampelakia Unit. This along with the top-SW shearing, suggest that the blueschist metamorphic event in both regions are one and the same (Walcott, 1998). The late greenschist and sub-greenschist top-NE shearing overprint is unique to the Pelion region as ductile deformation persisted until 15 Ma, whereas in the Olympos-Ossa region the ductile deformation was terminated at 36-40 Ma(Lips et al., 1999).

7 Conclusions

This study analysed the microstructures in thin sections of nappe contacts in the Olympos-Ossa, Pelion and Skiathos regions to understand the tectonic evolution of these regions with a focus on the CBU. The main findings of this study indicate that:

The samples from the Olympos-Ossa region showed a general top-SW directional shear sense, aligning with the high-pressure blueschist and greenschist-facies metamorphism that occurred between 64-36 Ma. With a plausible tectonic history of the CBU in region, as the Upper-CBU cut out the Middle- and Lower-CBU through the top-SW thrust.

The Pelion region exhibits both top-SW and top-NE shear senses reflecting the possible correlation with the top-SW shearing of the Olympos-Ossa region and the removal of the Lower Pelagonian Unit through the greenschist and sub-greenschist top-NE extensional faulting in the early Miocene.

The Upper Pelagonian and Eohellenic Nappe on Skiathos, which were tectonically stripped from the Pelion region, likely mirror the metamorphic conditions and deformational history of the units before their removal on Pelion.

Acknowledgements

I would like to express my gratitude to my supervisor, Uwe Ring for assigning me this project and introducing me to the wonderful intricacies of microstructures and its relation to large scale tectonics. I want to thank Alexandre Peillod for helping me with the identification of unknown minerals, and Yangbaihe Hong for her help in providing me some of her resources from her current PhD research. Lastly I would like to thank my family and friends for the continued support throughout the writing of this thesis.

References

Altherr, R., Kreuzer, H., Wendt, I., Lenz, H., Wagner, G.A., Keller, J., Harre, W., Höhndorf, A., 1982. A late Oligocene/early Miocene high temperature belt in the Attic-Cycladic crystalline complex (SE Pelagonian, Greece). Geol Jahrb Reihe E 23, 97–164.

Barker, A.J., 1998. Introduction to Metamorphic Textures and Microstructures. Routledge, London. https://doi.org/10.4324/9781315831626

Bucher, K., Grapes, R., 2011. Petrogenesis of metamorphic rocks (8th edition). Springer-Verl. Berl. Heidelb.

Eggleton, R.A., Banfield, J.F., 1985. The alteration of granitic biotite to chlorite. Am. Mineral. 70, 902–910.

Elmer, F., White, R., Powell, R., 2006. Devolatilization of metabasic rocks during greenschist–amphibolite facies metamorphism. J. Metamorph. Geol. 24, 497–513. https://doi.org/10.1111/j.1525-1314.2006.00650.x

Ernst, W.G., 1988. Tectonic history of subduction zones inferred from retrograde blueschist P-T paths. Geology 16, 1081–1084. https://doi.org/10.1130/0091-7613(1988)016<1081:THOSZI>2.3.CO;2

Evans, B.W., 1990. Phase relations of epidote-blueschists. Lithos, Third International Eclogite Conference 25, 3–23. https://doi.org/10.1016/0024-4937(90)90003-J

Ferentinos, 1973. The geology - petrology of the island of Skiathos. Bull. Geol. Soc. Greece 10, 323–358.

Ganne, J., Marquer, D., Rosenbaum, G., Bertrand, J.-M., Fudral, S., 2006. Partitioning of deformation within a subduction channel during exhumation of high-pressure rocks: a case study from the Western Alps. J. Struct. Geol. 28, 1193–1207. https://doi.org/10.1016/j.jsg.2006.02.011

Glodny, J., Ring, U., 2022. The Cycladic Blueschist Unit of the Hellenic subduction orogen: Protracted high-pressure metamorphism, decompression and reimbrication of a diachronous nappe stack. Earth-Sci. Rev. 224, 103883. https://doi.org/10.1016/j.earscirev.2021.103883

Godfriaux, I., 1968. Étude géologique de la région de l’Olympe (Grèce).

Graveleau, F., Malavieille, J., Dominguez, S., 2012. Experimental modelling of orogenic wedges: A review. Tectonophysics 538–540, 1–66. https://doi.org/10.1016/j.tecto.2012.01.027

Guiraud, M., Holland, T., Powell, R., 1990. Calculated mineral equilibria in the greenschist-blueschist-eclogite facies in Na2O−FeO−MgO−Al2O3−SiO2−H2O. Contrib. Mineral. Petrol. 104, 85–98. https://doi.org/10.1007/BF00310648

Harte, B., Graham, C.M., 1975. The Graphical Analysis of Greenschist to Amphibolite Facies Mineral Assemblages in Metabasites. J. Petrol. 16, 347–370. https://doi.org/10.1093/petrology/16.2.347

Hinshaw, E., Stockli, D., Soukis, K., 2024. Coherent underplating of HP-LT blueschist packages and basement during Hellenic subduction recorded by zircon U-Pb data, Pelion, Greece. J. Geol. Soc. 181. https://doi.org/10.1144/jgs2023-147

Hinshaw, E.R., Stockli, D.F., Soukis, K., 2023. Zircon and Apatite U-Pb Constraints on the Tectonic Affinity and Metamorphic History of the Blueschist-Facies Ambelakia Unit, Mt. Ossa, Greece. Tectonics 42, e2022TC007608. https://doi.org/10.1029/2022TC007608

Jacobshagen, V. (Ed.), 1986. Geologie von Griechenland, Beiträge zur regionalen Geologie der Erde. Gebr. Borntraeger, Berlin.

Jacobshagen, V., Wallbrecher, E., 1984. Pre-Neogene nappe structure and metamorphism of the North Sporades and the southern Pelion peninsula. Geol. Soc. Lond. Spec. Publ. 17, 591–602. https://doi.org/10.1144/GSL.SP.1984.017.01.46

Jolivet, L., Brun, J.-P., 2010. Cenozoic Geodynamic Evolution of the Aegean. Int. J. Earth Sci. 99. https://doi.org/10.1007/s00531-008-0366-4

Jolivet, L., Brun, J.P., Gautier, P., Lallemant, S., Patriat, M., 1994. 3D-kinematics of extension in the Aegean region from the early Miocene to the present; insights from the ductile crust. Bull. Société Géologique Fr. 165, 195–209.

Jolivet, L., Faccenna, C., Goffé, B., Burov, E., Agard, P., 2003. Subduction tectonics and exhumation of high-pressure metamorphic rocks in the Mediterranean orogens. Am. J. Sci. 303, 353–409. https://doi.org/10.2475/ajs.303.5.353

Kilias, A., 2024. The Alpine Geological History of the Hellenides from the Triassic to the Present—Compression vs. Extension, a Dynamic Pair for Orogen Structural Configuration: A Synthesis. Geosciences 14, 10. https://doi.org/10.3390/geosciences14010010

Kilias, A., 1995. Tectonic evolution of the Olympus-Ossa mountains: Emplacement of the blueschists unit in eastern Thessaly and exhumation of Olympus-Ossa carbonate dome as a result of Tertiary extension (Central Greece). Miner. Wealth 96, 7–22.

Kilias, A., Falalakis, G., Nastos, G., Mouintrakis, D., 1995. Tertiary extensional exhumation of the HP/LT Makrynitsa metamorphic core complex in Pelion mt. (eastern Thessaly).

Kilias, A., Fasoulas, C., Priniotakis, M., Sfeikos, A., Frisch, W., 1991. Deformation and HP/LT Metamorphic Conditions at the Tectonic Window of Kranea (W -- Thessaly, Northern Greece). Z. Dtsch. Geol. Ges. 87–96. https://doi.org/10.1127/zdgg/142/1991/87

Kogure, T., Banfield, J.F., 2000. New insights into the mechanism for chloritization of biotite using polytype analysis. Am. Mineral. 85, 1202–1208. https://doi.org/10.2138/am-2000-8-913

Laurent, V., Lanari, P., Naïr, I., Augier, R., Lahfid, A., Jolivet, L., 2018. Exhumation of eclogite and blueschist (Cyclades, Greece): Pressure–temperature evolution determined by thermobarometry and garnet equilibrium modelling. J. Metamorph. Geol. 36, 769–798. https://doi.org/10.1111/jmg.12309

Lips, A.L.W., White, S.H., Wijbrans, J.R., 1998. 40Ar/39Ar laserprobe direct dating of discrete deformational events: a continuous record of early Alpine tectonics in the Pelagonian Zone, NW Aegean area, Greece. Tectonophysics 298, 133–153. https://doi.org/10.1016/S0040-1951(98)00181-4

Lips, A.L.W., Wijbrans, J.R., White, S.H., 1999. New insights from 40Ar/39Ar laserprobe dating of white mica fabrics from the Pelion Massif, Pelagonian Zone, Internal Hellenides, Greece: implications for the timing of metamorphic episodes and tectonic events in the Aegean region. Geol. Soc. Lond. Spec. Publ. 156, 457–474. https://doi.org/10.1144/GSL.SP.1999.156.01.21

Lister, G.S., Banga, G., Feenstra, A., 1984. Metamorphic core complexes of Cordilleran type in the Cyclades, Aegean Sea, Greece. Geology 12, 221–225. https://doi.org/10.1130/0091-7613(1984)12<221:MCCOCT>2.0.CO;2

Magyarosi, Z., Watkinson, D.H., Jones, P.C., 2002. Mineralogy of Ni-Cu-Platinum-Group Element Sulfide Ore in the 800 and 810 Orebodies, Copper Cliff South Mine, and P-T-X Conditions during the Formation of Platinum-Group Minerals. Econ. Geol. 97, 1471–1486. https://doi.org/10.2113/gsecongeo.97.7.1471

Messiga, B., Tribuzio, R., Bottazzi, P., Ottolini, L., 1995. An ion microprobe study on trace element composition of clinopyroxenes from blueschist and eclogitized FeTi-gabbros, Ligurian Alps, northwestern Italy: Some petrologic considerations. Geochim. Cosmochim. Acta 59, 59–75. https://doi.org/10.1016/0016-7037(95)91549-9

Passchier, C.W., Trouw, R.A.J., 2005. Microtectonics. Springer Science & Business Media.

Peillod, A., Majka, J., Ring, U., Drüppel, K., Patten, C., Karlsson, A., Włodek, A., Tehler, E., 2021. Differences in decompression of a high-pressure unit: A case study from the Cycladic Blueschist Unit on Naxos Island, Greece. Lithos 386–387, 106043. https://doi.org/10.1016/j.lithos.2021.106043

Porkoláb, K., Willingshofer, E., Sokoutis, D., Creton, I., Kostopoulos, D., Wijbrans, J., 2019. Cretaceous-Paleogene Tectonics of the Pelagonian Zone: Inferences From Skopelos Island (Greece). Tectonics 38, 1946–1973. https://doi.org/10.1029/2018TC005331

Porkoláb, K., Willingshofer, E., Sokoutis, D., Wijbrans, J., 2020. Strain localization during burial and exhumation of the continental upper crust: A case study from the Northern Sporades (Pelagonian thrust sheet, Greece). Glob. Planet. Change 194, 103292. https://doi.org/10.1016/j.gloplacha.2020.103292

Ring, U., Glodny, J., Will, T., Thomson, S., 2010. The Hellenic Subduction System: High-Pressure Metamorphism, Exhumation, Normal Faulting, and Large-Scale Extension. Annu. Rev. Earth Planet. Sci. 38, 45–76. https://doi.org/10.1146/annurev.earth.050708.170910

Ring, U., Layer, P.W., 2003. High-pressure metamorphism in the Aegean, eastern Mediterranean: Underplating and exhumation from the Late Cretaceous until the Miocene to Recent above the retreating Hellenic subduction zone. Tectonics 22. https://doi.org/10.1029/2001TC001350

Ring, U., Pantazides, H., Glodny, J., Skelton, A., 2020. Forced Return Flow Deep in the Subduction Channel, Syros, Greece. Tectonics 39, e2019TC005768. https://doi.org/10.1029/2019TC005768

Schermer, E.R., 1993. Geometry and kinematics of continental basement deformation during the Alpine orogeny, Mt. Olympos region, Greece. J. Struct. Geol., The Geometry of Naturally Deformed Rocks 15, 571–591. https://doi.org/10.1016/0191-8141(93)90149-5

Schermer, E.R., 1990. Mechanisms of blueschist creation and preservation in an A-type subduction zone, Mount Olympos region, Greece. Geology 18, 1130–1133. https://doi.org/10.1130/0091-7613(1990)018<1130:MOBCAP>2.3.CO;2

Schermer, E.R., Lux, D.R., Burchfiel, B.C., 1990. Temperature-time history of subducted continental crust, Mount Olympos Region, Greece. Tectonics 9, 1165–1195. https://doi.org/10.1029/TC009i005p01165

Schmid, S.M., Fügenschuh, B., Kounov, A., Maţenco, L., Nievergelt, P., Oberhänsli, R., Pleuger, J., Schefer, S., Schuster, R., Tomljenović, B., Ustaszewski, K., van Hinsbergen, D.J.J., 2020. Tectonic units of the Alpine collision zone between Eastern Alps and western Turkey. Gondwana Res. 78, 308–374. https://doi.org/10.1016/j.gr.2019.07.005

van Hinsbergen, D., Hafkenscheid, E., Spakman, W., Meulenkamp, J.E., Wortel, M., 2005. Nappe stacking resulting from subduction of oceanic and continental Lithosphere below Greece. Geology 33. https://doi.org/10.1130/G20878.1

Vernon, R.H., 1986. Evaluation of the “quartz-eye” hypothesis. Econ. Geol. 81, 1520–1527. https://doi.org/10.2113/gsecongeo.81.6.1520

Walcott, C.R., 1998. The Alpine evolution of Thessaly (NW Greece) and late Tertiary Aegean kinematics/, Geologica Ultraiectina ; Utrecht University, Utrecht, The Netherlands:

Winkler, H.G.F., 1976. Classification Principles: Metamorphic Facies versus Metamorphic Grade, in: Winkler, H.G.F. (Ed.), Petrogenesis of Metamorphic Rocks. Springer, Berlin, Heidelberg, pp. 55–63. https://doi.org/10.1007/978-3-662-22283-6_6

Winter, J.D., 2014. Principles of igneous and metamorphic petrology, 2. ed., Pearson new internat. ed. ed. Pearson Education, Harlow.

Yarwood, G., Dixon, J., 1977. Lower Cretaceous and younger thrusting in the Pelagonian rocks of the High Pieria, Greece.

Appendix

Appendix A: Mineral abbreviation

Abbreviation	Full Name
Act	Actinolite
Aug	Augite
blue Amp	Blue Amphibole
Bt	Biotite
Cal	Calcite
Chl	Chlorite
Dol	Dolomite
Ep	Epidote
Fsp	Feldspar
Hbl	Hornblende
Opq	Opaque Mineral
Qz	Quartz
Stp	Stilpnomelane
Tr	Tremolite
Ttn	Titanite
Wm	White Mica

Appendix B:Fullscans of thin sections

Every fullscan of the thin sections that were not mentioned in the results.

Link to Google Drive Folder with TIFF files:

https://drive.google.com/drive/folders/1hoWU2SYOcK4Vsp0jzdBzHI2nble6E04L?usp=sharing